

STARS

University of Central Florida
STARS

Electronic Theses and Dissertations, 2004-2019

2012

Process Optimization Towards The Development Of An Automated Cnc Monitoring System For A Simultaneous Turning And Boring Operation

Manuel Hernandez
University of Central Florida

 Part of the [Mechanical Engineering Commons](#)

Find similar works at: <https://stars.library.ucf.edu/etd>

University of Central Florida Libraries <http://library.ucf.edu>

This Masters Thesis (Open Access) is brought to you for free and open access by STARS. It has been accepted for inclusion in Electronic Theses and Dissertations, 2004-2019 by an authorized administrator of STARS. For more information, please contact STARS@ucf.edu.

STARS Citation

Hernandez, Manuel, "Process Optimization Towards The Development Of An Automated Cnc Monitoring System For A Simultaneous Turning And Boring Operation" (2012). *Electronic Theses and Dissertations, 2004-2019*. 2134.

<https://stars.library.ucf.edu/etd/2134>



PROCESS OPTIMIZATION TOWARDS THE DEVELOPMENT OF AN
AUTOMATED CNC MONITORING SYSTEM FOR A
SIMULTANEOUS TURNING AND BORING OPERATION

by

MANUEL HERNANDEZ
B.S. University of Central Florida, 2010

A thesis submitted in partial fulfillment of the requirements
for the degree of Master of Science in Mechanical Engineering
in the Department of Mechanical, Materials, and Aerospace Engineering
in the College of Engineering and Computer Science
at the University of Central Florida
Orlando, Florida

Spring Term
2012

©2012 Manuel Hernandez

ABSTRACT

Manufacturing operations generate revenue by adding value to material through machine work and the cost associated with part production hinders the maximum profit available. In order to remain competitive, companies invest in research to maximize profit and reduce waste of manufacturing operations. This results in cheaper products for the customer without sacrificing quality. The purpose of this research was to identify machine settings of an Okuma LC 40 Turning Center and optimize the cost of machining in terms of tool cost and energy consumption while maintaining part quality at a productive cycle time. Studying the relationship between energy consumption, tool life, and cycle time with the speed and feed settings through statistical Analysis of Variance (ANOVA) method will allow the production plant to make profitable financial decisions concerning simultaneous turning operation of forged chrome-alloy steel. The project was divided into three phases; the first phase began with a literature survey of sensors used in current manufacturing research and the adaptation of our sensors to the Okuma LC 40 turning center. Then, phase II used design of experiments to identify spindle speed and feedrate settings that optimize multiple responses related to the turning process. The result was a saving in energy consumption (kWh) by 11.8%, a saving in cutting time by 13.2% for a total cost reduction from \$1.15 per tool pass to \$1.075 per tool pass. Furthermore, this work provides the foundation for phase III to develop an intelligent monitoring system to provide real-time information about the state of the machine and tool. For a monitoring system to be implemented in production, it should utilize cost effective sensors and be nonintrusive to the cutting operation.

TABLE OF CONTENTS

LIST OF FIGURES.....	vi
LIST OF TABLES	viii
LIST OF ABBREVIATIONS.....	ix
CHAPTER ONE: INTRODUCTION	1
CHAPTER TWO: BACKGROUND	5
Design of Experiments	5
Steps for Design of Experiment Studies	9
Plan the Experiment.....	10
Design the Experiment.....	12
Perform Experiment Runs.....	14
Analyze Data and Draw Conclusions	15
CHAPTER THREE: PHASE I EXPERIMENT SETUP	18
CNC Turning Experiment Platform	18
Sensor Information	23
CHAPTER FOUR: PHASE II DESIGN OF EXPERIMENT	29
Experimental Design and Evaluation	29
Tool Life Study	40
CHAPTER FIVE: OPTIMIZATION AND VALIDATION DISCUSSION	48

CHAPTER SIX: CONCLUSION	57
REFERENCES.....	58

LIST OF FIGURES

Figure 1: Learning Curve and Break Even Line	6
Figure 2: General Model of the CNC Turning Process	8
Figure 3: Image of 4137 Chrome Alloy Steel Workpieces	11
Figure 4: Experiment Space.....	13
Figure 5: Kennametal OD Tool Insert.....	18
Figure 6: A 2-D sketch of AISI 4137 Steel Workpiece.....	19
Figure 7: Experiment Setup	20
Figure 8: Sensors of lower turret.....	20
Figure 9: Sensors of upper turret.....	21
Figure 10: DAQ Setup Diagram	22
Figure 11: Flow Chart of Data through the Producer-Consumer Architecture	23
Figure 12: Dynamometer and Adapter Plate	24
Figure 13: Adapter plate with Force Sensors.....	25
Figure 14: Boring Bar with Adapter Plates and Sensors	25
Figure 15: Groove Location for Thermocouple on Insert	26
Figure 16: Power Meter in Electrical Cabinet	27
Figure 17: Microphone Setup	28
Figure 18: DoE Design Space.....	31
Figure 19: DoE Analysis and Model Fitting.....	33
Figure 20: Main Effects Plot of Average Power.....	34
Figure 21: Pareto Chart of the Significant Effects for Anverage Power	36

Figure 22: Plot of Residual Results for Final ANOVA Regression.....	38
Figure 23: Turning Tool Wear Microscope Pictures for pass #1, #7, #14, #19	41
Figure 24: Flank Wear versus Tool Pass Number	43
Figure 25: Power at Different Factors versus Material Removed	44
Figure 26: Waterfall plot of Microphone PSD at Factory Settings.....	46
Figure 27: Surface Plot of Tool Cost.....	49
Figure 28: Overlaid Contour Plot of Cost and Other Responses	50
Figure 29: Optimal Settings from Response Optimizer	51
Figure 30: Functional Diagram of Monitoring System	56

LIST OF TABLES

Table 1: Response Surface II Experiments for Simultaneous OD Turning and ID Boring	32
Table 2: Minitab ANOVA Analysis Table for Average Power.....	35
Table 3: Estimated Regression of Average Power with Updated Terms	37
Table 4: Comparison of Regression Equation to RS III.....	39
Table 5: Main Effects of Other Response Averages	40
Table 6: Experiment Runs	42
Table 7: ID Prediction Results	43
Table 8: Comparison of Results to	52

LIST OF ABBREVIATIONS

AISI.....	American Iron and Steel Institute
AE.....	Acoustic Emissions
ANOVA.....	Analysis of Variance
CNC.....	Computer Numerical Control
DoE.....	Design of Experiments
EDA.....	Exploratory data analysis
FFT.....	Fast Fourier Transform
ID.....	Inner Diameter
IPR.....	Inches per revolution
MRR.....	Material Removal Rate
OD.....	Outer Diameter
RMS.....	Root Mean Square
RPM.....	Revolutions per minute
TTL.....	Taylor Tool Life

CHAPTER ONE: INTRODUCTION

Manufacturing operations generate revenue by adding value to material through machine work, and the cost associated with part production hinders the maximum profit available. In order to remain competitive, companies must continuously optimize production operations to reduce waste and managing cost. The result is cheaper products for the customer without sacrificing quality. Optimizing the cost of CNC turning is the primary motivation for conducting the research presented in the following chapters.

To achieve CNC cost reduction it is imperative to identify a range of settings which will balance tool cost and energy consumption while maintaining part quality at a productive cycle time. The Okuma LC-40 Turning Center has two turrets and is capable of high production rates when utilizing both turrets to remove material in a simultaneous turning and boring operation. Understanding the relationship between energy, tool life, and cycle time with machine settings will allow the production plant to make profitable financial decisions concerning the simultaneous turning of AISI 4137 forgings. Machine Plant managers may take advantage of the data and utilize the most profitable machines or even investigate why some machines are not performing efficiently. Furthermore, studying these relationships will make up the backbone of a monitoring system to provide real-time information about the current machining cost as well as tool life.

In the introduction and background chapter, the paper focuses on results from Phase I of the project. The goal of Phase I was to survey various sensors for manufacturing machine research and equip sensors to our Okuma LC 40 CNC. Phase II of the project focused on offline

analysis of sensor data to optimize multiple responses over the current conditions implemented in the factory. The design of experiment (DoE) method was implemented to gather data as well as characterize the tool according to the Taylor Tool Life model. This research also presents the foundation plans for online control of machining cost and tool life of Phase III. This includes the development of a program diagram for Labview control program and results from hardware testing of the CNC override system with a microcontroller.

The manufacturing industry recognizes that research will spur advancements in machine tool monitoring systems which empower them to make intelligent decisions and interact with human operators. Many machine tools already have some sort of monitoring systems which halt operations if safety checks conditions are not met; such as indicator lights for low pressure or fluid levels. Though these systems exhibit some basic sensing and monitoring behavior, they do not function to enhance the machines efficiency or productivity. In order to advance CNC systems researchers investigate tool wear and chatter by monitoring states with time series domain, frequency domain, and wavelet methods [1-3]. The research into CNC machine monitoring has formed concentrations into areas such as tool condition monitoring, condition based maintenance, and chatter detection [4-8].

Researchers working towards tool condition monitoring aim to develop techniques which will give insight to the tools status. The ability to predict tool failures will prevent ruined surface finishes from tool breaks during cutting as well as the additional machine work to correct ruined surfaces. In some instances, the damage from tool breaks may not be correctable, and the workpiece must be scrapped - at high cost to the manufacturer. Li [9] presents a comprehensive

review on the use of acoustic emissions (AE) to monitor tool wear during turning operations. According to ASTM E610-77, Acoustic emission is the class of phenomena whereby transient elastic waves are generated by the rapid release of energy from localized sources within a material, or the transient elastic waves so generated. Sensors for tool wear monitoring have been classified into direct and indirect sensing methods, depending on the sensor. Direct sensing methods include optics and electrical resistance; indirect sensing methods include acoustic emissions motor current, cutting force and vibrations[9]. Indirect sensing methods are the focus of the study presented in this thesis. The advantage of AE for tool condition monitoring is the high frequency range that is above the machine vibrations and noise in the environment. Additional to using indirect sensing methods of AE, cutting force, sound, vibration, power, and temperature; the method of decomposing and interpreting the signal is just as important as the type of sensor[10]. Analyzing metrics such as average power, average force, and AE root mean square (RMS) from the time series reveals trends with the wear of the tool. The frequency response from a microphone and an accelerometer signal has also proven effective for providing insight to the state of the tool during the turning process [3, 11]. A variety of sensors have been employed to study machine cutting: forces, power, AE, vibrations, sound, and temperature. After a sensor is selected and adapted to the machine, it is coupled with signal processing methods such as time domain metrics, Fast Fourier Transform (FFT) analysis or wavelet analysis[12].

This thesis focuses on the time series metrics of the cutting forces, power and temperature as the responses for a DoE study to optimize the machine settings. Additionally, the FFT of acceleration and audible sound signal are analyzed to investigate tool life trends. Using data from DoE studies provides essential information to develop a scheme for CNC monitoring

system. By utilizing multiple sensors, the monitoring system may fuse data and provide complementary information about changes in the tool and machine condition [13]. The sensors for this research have been selected on the basis of correlational studies; the power meter can suggest trends similar to cutting forces and the microphone may show strong relation to the cutting vibration signal. Dey and Stori remark that the practicality of using sophisticated dynamometer force sensors in industrial settings is minimal due to the high cost and intrusive nature of the sensor [10]. The cables of the turning force dynamometers limit the machine's ability to rotate multi-tool turrets and perform multiple operations. At the end of analyzing the DoE study data, the proposed monitoring system will utilize an inexpensive power meter and microphone adapted to the machine's standard factory configuration so that machining cost and tool life may be monitored.

CHAPTER TWO: BACKGROUND

Design of Experiments

In England, Ronald A Fisher pioneered Design of Experiments (DoE's). Fisher's purpose was to improve crop yield by studying the different influencing factors on agriculture [14, 15]. His method of systematically designing experiments and analyzing the variance did not only influence agriculture, but other fields such as psychology and various levels of engineering [16]. William E. Deming and Dr. Genichi Taguchi are best known for employing the DoE statistical method in modern manufacturing for continuous process improvement and quality control [17, 18]. According to Condra, "DoE's is a method of systematically obtaining and organizing knowledge so that it can be used to improve operations in the most efficient manner possible [18]." In this sense, experimental designs can be implemented in any organization at any level with the goal of gaining a better understanding of a relationship between the inputs and outputs of a certain process. DoE's play a major role in manufacturing processes; from optimizing the production process of microelectronic devices to the characterization of material strength based on composition factors [18].

In the manufacturing of goods, the goal has always been to make products faster with little waste to yield maximum profit and out last competitors. Figure1, depicting a typical manufacturing learning curve, illustrates the objective of using designed experiments to ensure success. The y-axis is yield, or profit, as a function of time or production volume. The blue line represents the learning curve of the manufacturing process and the red dashed line is the minimum yield, or profit, to achieve break even. The two regions, A and B represent critical

areas for companies to focus the efforts of their operations. Area A is at the beginning of production, maybe a new product line. It is crucial for them to reduce the area of A and meet break even quickly. The most profit is achieved by reaching B quickly and constantly improving to create a large difference between yield from manufacturing and break even [18]. The studies being presented directly influence Area B, where the process has already been established and research is conducted to maximize the profit over the current turning operation. In general, the DoE method is used as a tool to gauge how machining cost, tool life, and energy consumption are affected by the CNC spindle speed and feed settings.

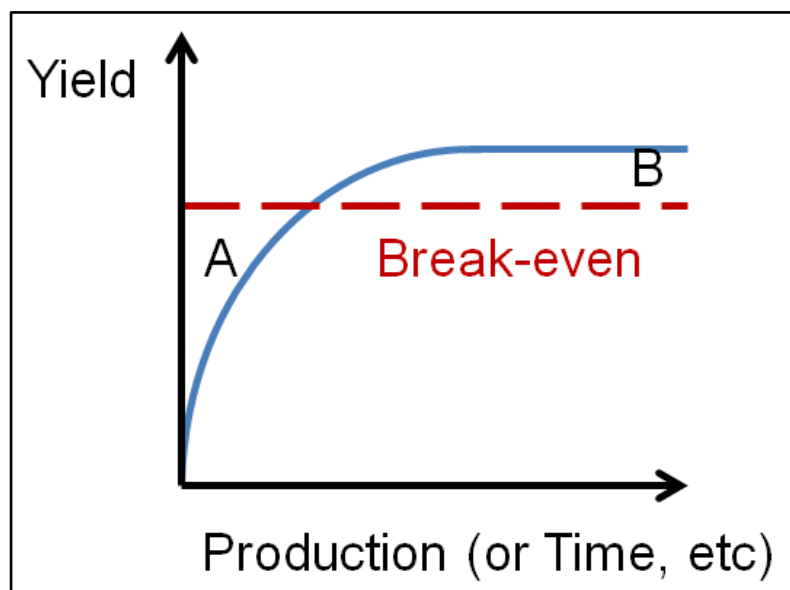


Figure 1: Learning Curve and Break Even Line

There are numerous benefits from using the DoE method over traditional method of changing one factor at a time. Several factors of the process are optimized simultaneously by systematically exploring combinations of levels. This result is the same realized information with less number of experiments than the traditional one-at-a-time method. Both time and money may

be saved by conducting a DoE than by looking at one factor at a time. Another benefit of using DoE is that it considers noise in the machining process. When looking at only one factor at a time, the noise may be overlooked. In DoE studies, the noise is incorporated into the process and is optimized regardless of noise allowing for robust parameters to be selected. A sense of control is realized because the effect of a cause of variation is eliminated without directly eliminating the cause [18].

Now that the background and usefulness of the DoE method have been established, the fundamental DoE concepts will be emphasized in regards to the CNC turning study. The fundamental black box method is utilized in many texts to illustrate the inputs and outputs of the process. Figure 2 is a representation of variables involved in the CNC turning process. The input variables being controlled in the studies presented include the spindle's revolution per minute (RPM), the feedrate in inches per revolution (IPR), and the depth of cut for the outer diameter (OD) turning tool and inner diameter (ID) boring tool. The depth of cut is programmed into the g-code in order to bring the part into specification for the final finishing pass. In the production environment, the machinist is able to adjust the spindle RPM and feedrate during the process with mechanical switches on the CNC control panel. The machinist will adjust the settings if chatter or tool wear is observed.

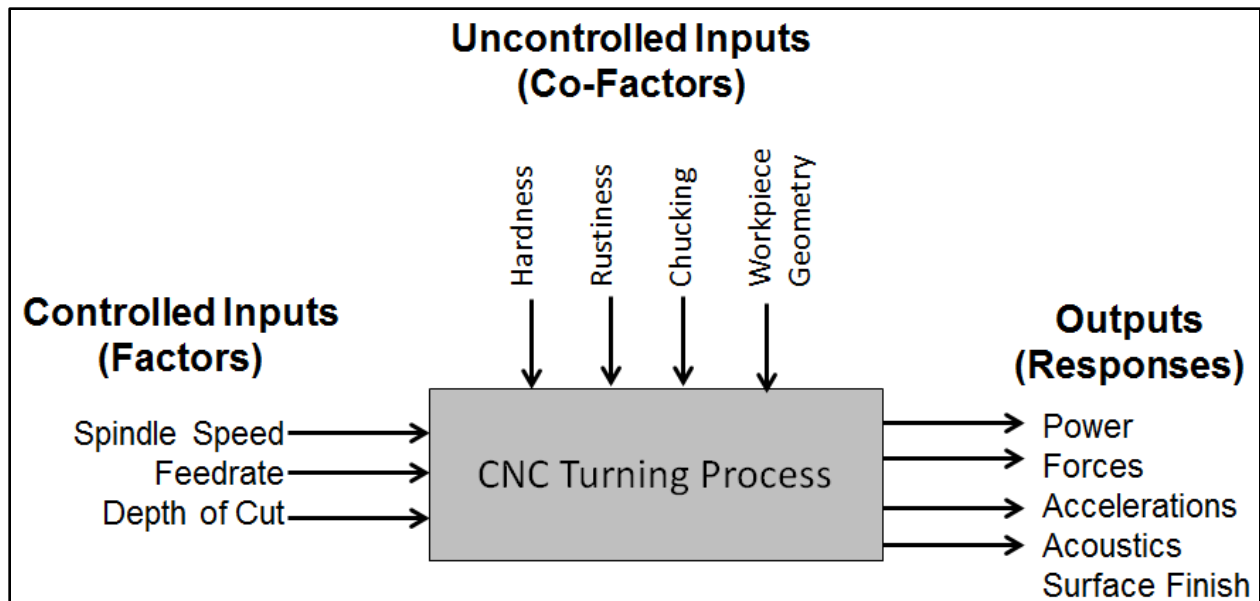


Figure 2: General Model of the CNC Turning Process

While touring a production facility, it was noted that machinists listen for abnormal noises and visually inspect the tool after the roughing operations have finished. In the DoE studies presented, the output responses will be measured with sensors. A microphone will be used to record audible noises from the machining. Because machinists rely on their sense of hearing to determine abnormal conditions, the microphone will be investigated to determine if it is capable for use in robust detection of tool wear. Studies suggest that tool chatter, which exhibits excessive vibrations, diminishes surface finish. It is important that the surface finish from the roughing process be within the acceptable tolerance range for the finishing process. As the tool passes the metal surface there is a wavy indentation from the tool vibration that will influence the finishing pass [19]. To ensure specification of the finish, the surface finish is measured with a surface roughness meter, which passes over the machined surface and measures the deflection in microns. The amount of vibrations and audible signal are investigated to

determine any correlation between each other and surface finish. Further, DoE studies are conducted to determine if the accelerometer and the microphone sensor show any relation to tool wear.

The uncontrollable factors, known and unknown, account for noise in the process [16, 18, 20]. Uncontrollable factors, which are able to be measured in the study, include the outer diameter surface hardness of the 4137 chrome alloy steel, a qualitative measure of the amount of rust, and eccentricity of the inner diameter to outer diameter. The outer diameter surface hardness is measured using a portable Leeb hardness tester. The variation in workpiece eccentricity is gauged by measuring the wall thickness around different locations with calipers. Rust is gauged by the experimenter on three descriptive levels from little, moderate, to extreme rust.

Steps for Design of Experiment Studies

This section of the paper will emphasize the four steps of the DoE studies in relation to CNC turning experiments. The first step is to plan the experiment: identify the objectives, determine the process variables, and levels of the input variables. The second step is to design the experiment: based on the objectives and previous observations of the variables, determine which experiment design should be employed. The third step is to perform the experiment: ensure all procedures have been documented according to the experiment plan. The last step is to analyze the data and draw conclusions [16]. Each step is equally important because performing each step properly is necessary for a successful completion of the study objectives.

Plan the Experiment

In planning an experiment, the experimenters need to consider the purpose for conducting the experiment. Also, the objectives for an experiment should be practical in nature. Are the experimenters seeking to maximize a response like quality, profit or strength? Typically there is a response output of interest from the process in question and the desire is to maximize, minimize, or hit a target value [18]. The objective of the first DoE study is to screen main effects of the temperature near the tool, turning forces, power, accelerations, and microphone acoustics for a simultaneous OD and ID operation of 4137 chrome alloy steel, figure 3.



Figure 3: Image of 4137 Chrome Alloy Steel Workpieces

It was decided that the input factors for the first DoE study include the spindle RPM, the feedrate IPR, depth of cut (DOC) OD and DOC ID. The uncontrollable factors in the experiment would be the hardness of the workpiece. The amount of rust and eccentricity variation of workpiece geometry would be negated by performing a “cleaning pass” on the rusty outer and inner surfaces. Each controllable factor input was given two levels around current factory settings; twenty percent above and below. The factory settings were used as center points in the experiments. The factory set spindle speed is 350 RPM, thus making the low level 280 RPM and the high level 420 RPM. The standard feedrate used in the factory is 0.020 IPR, thus making the low feedrate level 0.016 IPR and the high level 0.024 IPR. The center point DOC for OD and ID

was 0.160 inches. Twenty percent above and below the centerpoint DOC is 0.200 inches and 0.120 inches. It should also be noted that the depth of cut is in terms of radius.

A highlight of the first study was the optimized machine settings in the 280-420 RPM range and 0.016-0.024 IPR range with respect to energy consumption and cycle time. The energy consumption is a variable in the machining cost objective function. To observe the impact of tool cost in the cost equation, another study was conducted to characterize the tool life according to the Taylor Tool Life (TTL) equation. The TTL equation is an exponential function of cutting speed and feedrate to estimate the life in minutes of a tool [21-23]. The input variables for the known TTL model are surface speed of the cutter and feedrate. The response is the amount of time until the tool wear is greater than 0.5 millimeters. A microscope is used to characterize the amount of flank wear on the carbide cutting tool insert. Then, settings are chosen by optimizing the cost of machining with respect to energy consumption, tool cost, and cutting time. The surface speed settings were set at 183.073 m/min and 219.688 m/min. The feedrate settings were 0.5080 mm/rev and 0.6096 mm/rev.

Design the Experiment

After the objectives for the experiment have been established, and the responses of interest are selected, it is then necessary to select the type of experimental design. A full factorial Design of experiment is performed with combinations of every factor level. For a two level full factorial design of experiment, with n number of factors, there are 2^n number of test runs. If there are two factors: spindle speed and feedrate, with 2 levels each, then the number of experiments in the DoE is four. Center points may be added to the design space to check for

curvature in the process and to provide a way to measure variability in the process; possibly due to time or some other unknown factor [24]. Additional axial points may be added to the design space and create a response surface design experiment. The left image of Figure 4, displays experimental space for a 2 level, 2 factor full factorial design of experiment. The right image of figure 4, displays a response surface design of the same spindle speed and feedrate factors. The axial points lie on the center of the faces of the square, making it a Face Centered Design. The response surface design allows for further analysis of interaction effects to optimize machine process settings. Extra data points in response surface designs allow for estimations of second order interaction effects [25]. The Face Centered Response Surface Design is used in the four factor investigation and optimization of the simultaneous turning and boring operation. Only extreme points of the region are being used to fit the known model of tool life.

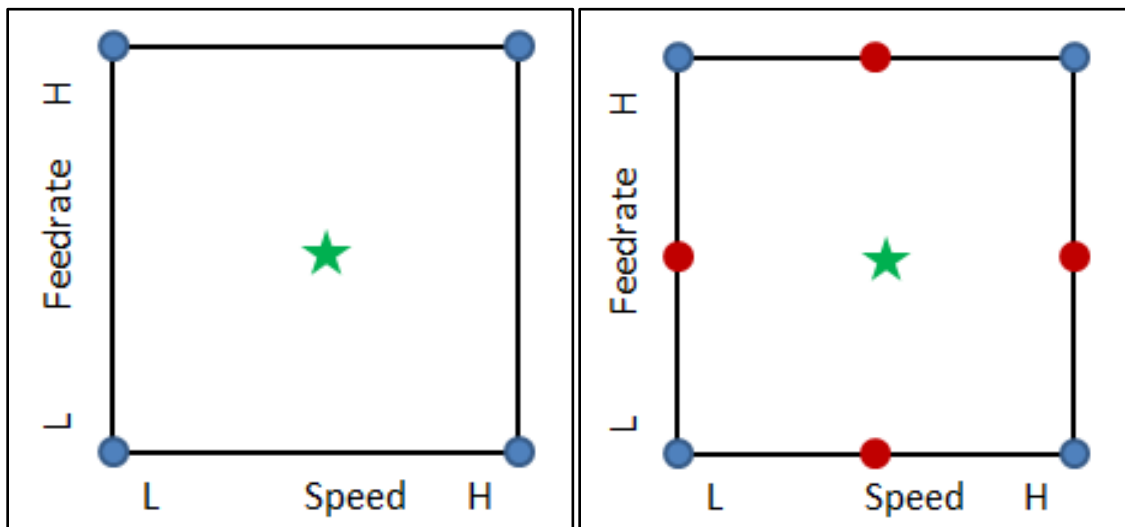


Figure 4: Experiment Space

Perform Experiment Runs

The next step is to perform the experiment runs in the DoE study. Prior thoughts of the steps needed to complete an experiment run must be noted so that as much of necessary data is gathered without mistakes. Following an experiment procedure will also ensure data is unbiased and does not overlook any known uncontrollable factors, which may lead to the process not being robust. For example, if the flow rate for metal working fluid is checked before each experiment for proper flowing conditions, then this must be duplicated in the production scenario. If the metal working fluid is not flowing than the DoE study is not able to account for factors outside of the parameters under investigation. The lack of metal fluid flow will result in less chip removal, creating more heat around the cutting zone and wearing the tool faster. It is understood that numerous factors may not be measurable and if unexpected variations result, noting as much detail about the experiment as possible will give rise for suspects to investigate.

To ensure proper and complete collection of data, experiment procedures are documented with an Experiment Worksheet. The Experiment Worksheet is a guideline created before running the experiment to display all of the steps and checks to ensure each run is uniformly executed. To some extent, the Experiment Worksheet sterilizes the DoE, but optimal results will be robust in the sense of the factors accounted for on the Experiment Worksheet. The Experiment Worksheet requires names of those conducting the test run as well as the time and date the test took place. The experimenters are also required to sign their initials in boxes next to procedures in order to ensure responsibility for completing the task. Tasks on the Experiment Worksheet include: checking the condition of sensors, loading and labeling workpieces, documenting and loading tooling and recording pre-test offline data.

The Experiment Worksheet is a Microsoft Word document that is linked to a Microsoft Access database. The Access database stores all test information for every run in the DoE. Linking the Access database to the Experiment Worksheet Word document allows for easy input of run number and machine settings to be used in the test. The checking of the machine settings in the g-code is another task that needs to be included in the Experiment Worksheet. The worksheet also contains pre-test information such as wall thickness measurements for eccentricity and qualitative description of the amount of rust. Post-test offline data includes qualitative description of tool condition, recorded measurements of surface finish, outer diameter hardness and qualitative description of the chip color and formation.

Analyze Data and Draw Conclusions

Experimental designs are an exploratory data analysis (EDA) approach [24]. This approach utilizes graphical representation of data to explore and provide insight on the trends of various responses [26]. Graphical representations of data include main effects plots, to show trends over the factors, and interaction plots, which reveal interactions among the factors, and probability plots, to observe the distributions of data. The main effect plot, displays the response values over each factor, typically a large change in the response value indicates that the factor was significant in changing the response. Interaction plots are useful because they can be used to show how a response variable relates to other factors. It plots the response of each level of a factor with the level of a second factor held constant. Interaction of the factors will be revealed if the response over a factor differs greatly for the second factor. If the trends in the interaction plot

do not appear similar, then an interaction is present. Pareto charts are also employed to determine the importance of factors for a particular response.

After graphically analyzing significant factors amongst the plots, models may be created using the analysis of variance. The ANOVA model will predict a particular response in terms of the significant factors. The ANOVA process has two parts, the regression to fit a model to a response as a function of the input factors, and also hypothesis testing to see how well the model fits the data. After the non-significant factors are removed from another iteration of analysis, the least squares regression is used to develop a more accurate model of the response. Unlike collocation, where a function is fit to pass every data point, regression is a method to obtain the best fit to a set of data. The least squares regression model aims to develop coefficients which reduce the error from the model to the observed. This regression method may be used to approximate linear or higher order polynomials to a data set [27]. There are many statistical software which can perform the least squares, ANOVA calculations, and present graphical representation of data [18]. Minitab 16 was selected to perform the data offline analysis. More description of ANOVA tables are presented in Myers and Montgomery [25] and other DoE text [16, 18, 28]. Optimal settings may then be chosen according to a well fit model of the power consumption and other key responses.

The other goal of the research study was to determine the effect of tool cost on the machining cost. Tool life studies were run in order to fit the TTL equation, Equation 1. The constants in the equation, C , m , and n , may be determined with three runs. Each run had a different combination of cutting speed and feedrate with the response being tool life in minutes.

$$T(\text{minutes}) = C * v^m * f^n \quad (1)$$

The TTL equation is a variable in the overall cost of machining. Equation 2 is the proposed cost function adapted from Salvendy and Tlustý [29, 30]. It defines the cost to remove a certain amount of material as a function of the machinist costs, the costs associated with the tool, and the cost of energy. The tool cost factor is driven by the tool life which has an inverse relation with the material removal rate. The function is useful for observing the change in total cost as constants such as energy cost or tool cost change. Additionally, there is the advantage of optimizing the settings over key responses that make up the cost of machining.

$$Cost = \left(EC * P * \frac{t_m}{60} \right) + \left(\frac{C_{te}}{TTL} * \frac{V}{MRR} \right) + (t_m * r_m) \quad (2)$$

Cost	Cost to remove specific volume of material
<i>EC</i>	EC is the going rate of energy for the plant (\$/kWh)
<i>P</i>	Average power in kW
<i>t_m</i>	Machining time in minutes
<i>r_m</i>	Rate of machining
<i>C_{te}</i>	Cost per tool edge
TTL	Taylor Tool Life equation (a function of speed and feed)
<i>V</i>	Volume in cubic inches of material removed
<i>MRR</i>	Material Removal Rate (in.cu./min.)

CHAPTER THREE: PHASE I EXPERIMENT SETUP

CNC Turning Experiment Platform

The experiments for the turning operations were carried out on an Okuma LC-40 turning center with Kennametal CNMG544RP 9110 tool inserts for OD turning and SNMG644RN KC9140 of ID boring. A three jaw hydraulic chuck was used to clamp the workpiece. The AISI 4137 forged steel workpieces measure approximately 20.5 in long by 6.9 in. A 2-D sketch of the workpiece geometry is shown in Figure 6; the workpiece resembles a cylinder with outer diameter of 6.9 in with a 17 in. deep, 3 in. diameter bore. One end, denoted left in Figure 6, is chamfered down to a diameter of 5.5 in.



Figure 5: Kennametal OD Tool Insert

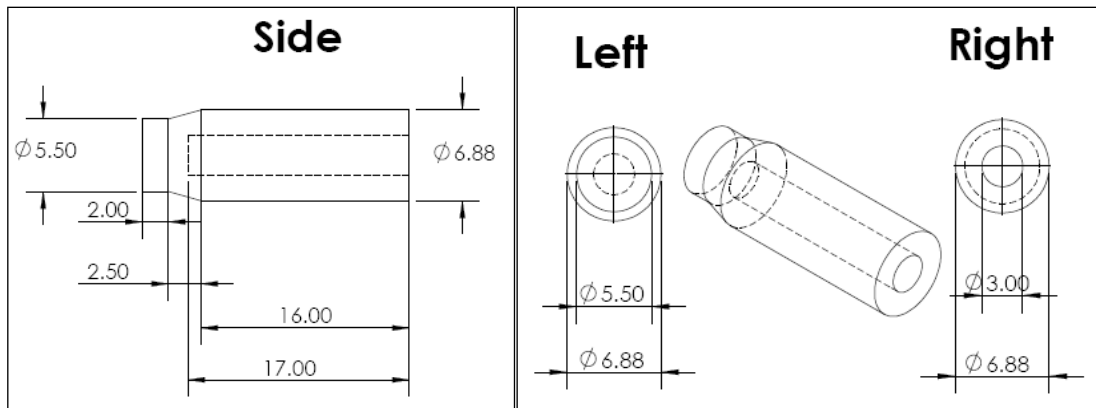


Figure 6: A 2-D sketch of AISI 4137 Steel Workpiece

The OD turning experiments were carried out by the lower turret of the lathe. Another operation under investigation was simultaneous material removal from turning and boring. Simultaneous operations synchronize the upper turret for ID boring with the lower turret for OD turning. The advantage of combining operations with both turrets is reduced machining time.

The sensors equipped to the Okuma CNC are classified to shared and turret sensors. The shared sensors consist of the power meter, microphone, flow meter, and metal working fluid thermocouple, which are considered shared because their responses are not dependent on which turret is used during the machining operation. Figure 7 illustrates the flow of turret specific and shared sensor information to the data acquisition system.

All of the turret sensors are either mounted to the upper turret or to the lower turret and measure similar stimuli during machining. Mounted to the lower turret turning assembly are: a dynamometer, accelerometer, acoustic emissions sensor and thermocouple. The upper turret boring assembly is equipped with the same types of sensors, with the exception of a set of four

force sensors. Detailed mounting descriptions of sensors are provided in a later section. Figure 8 and 9 depict the routing of each turret's sensor information to the DAQ system.

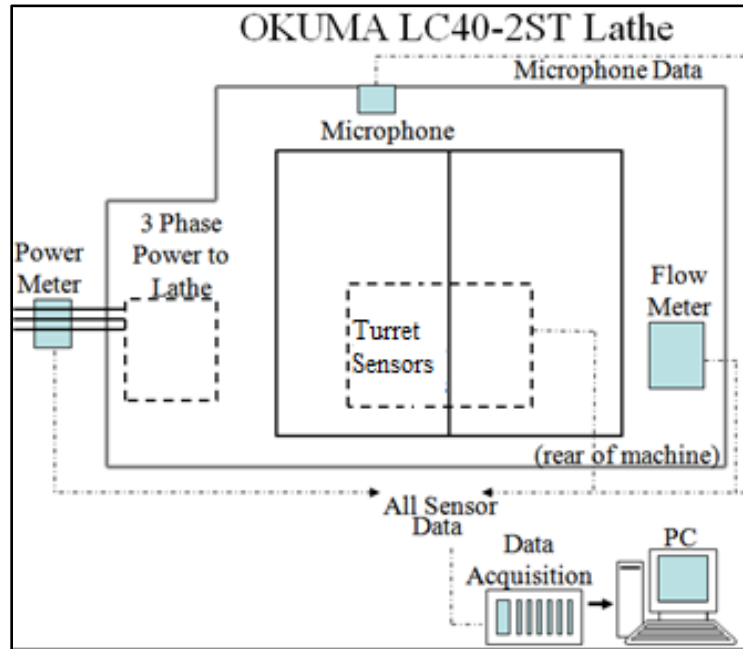


Figure 7: Experiment Setup

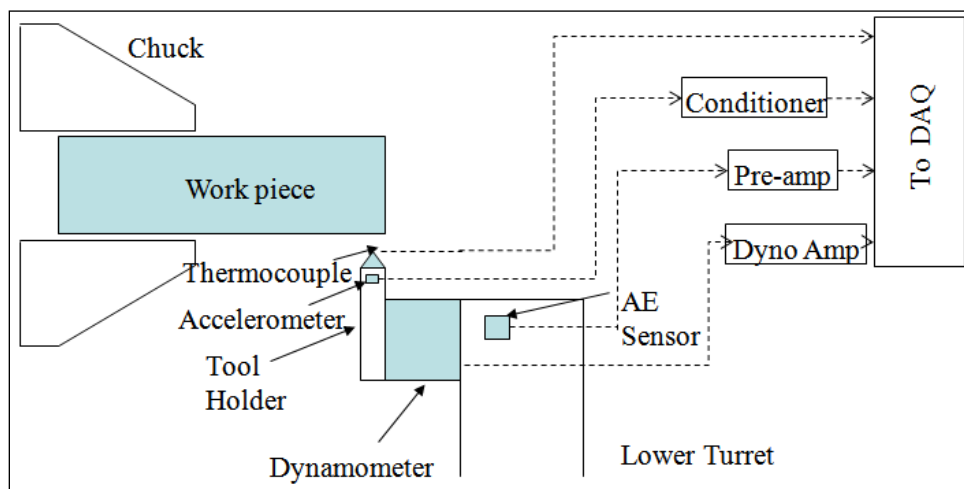


Figure 8: Sensors of lower turret

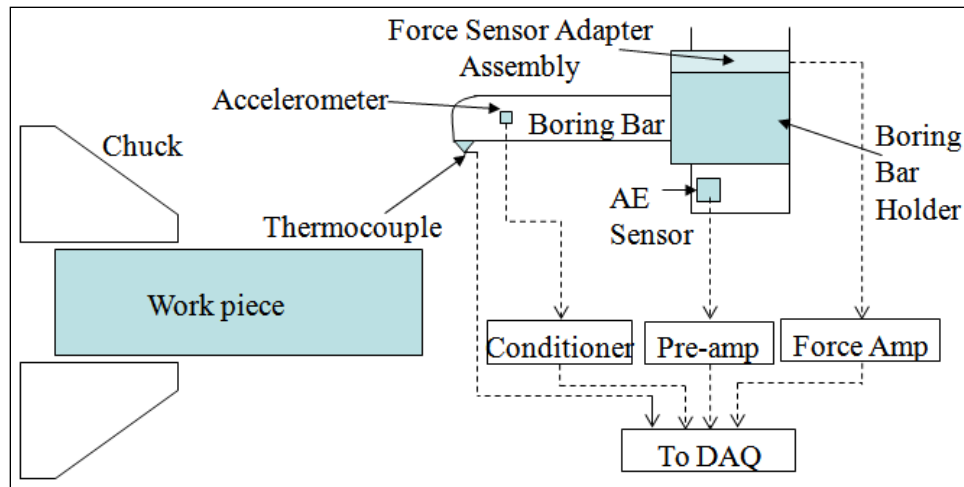


Figure 9: Sensors of upper turret

The lathe is equipped with a total of twelve sensors that are directed to the National Instruments PXI data acquisition system. A diagram illustrating the complete sensor set up is shown in Figure 10. The DAQ system consists of a PXI-1042 Chassis with a PXI-8108 embedded controller. Labview Real-time OS runs a Producer-Consumer program to acquire simultaneous data at various rates. In the producer/consumer architecture, two separate timed loop structures operate at different rates: one or more ‘producer loops’ acquire data from the hardware buffer on the DAQ card at a deterministic rate, and store that data into an ‘RT FIFO buffer’ on the PXI controller motherboard; a separate ‘consumer loop’ transfers data from the RT FIFO buffer on the PXI controller to a file on the hard disk. Because writing to a hard disk is a nondeterministic process (there is no upper limit on the amount of time it will take to write data to a hard disk), the consumer loop cannot be iterated at a deterministic rate. Also, the deterministic data acquisition task is separated from the nondeterministic data write task, so the data can be collected at a deterministic rate necessary for reliable data acquisition, and written to

the hard drive immediately. A flowchart showing the path of data through the producer/consumer architecture is shown below in Figure 11. The DAQ program was started before the machining process and continued until the spindle and axis stopped. A separate Labview program on the host computer analyzed the offline data from every signal in each run.

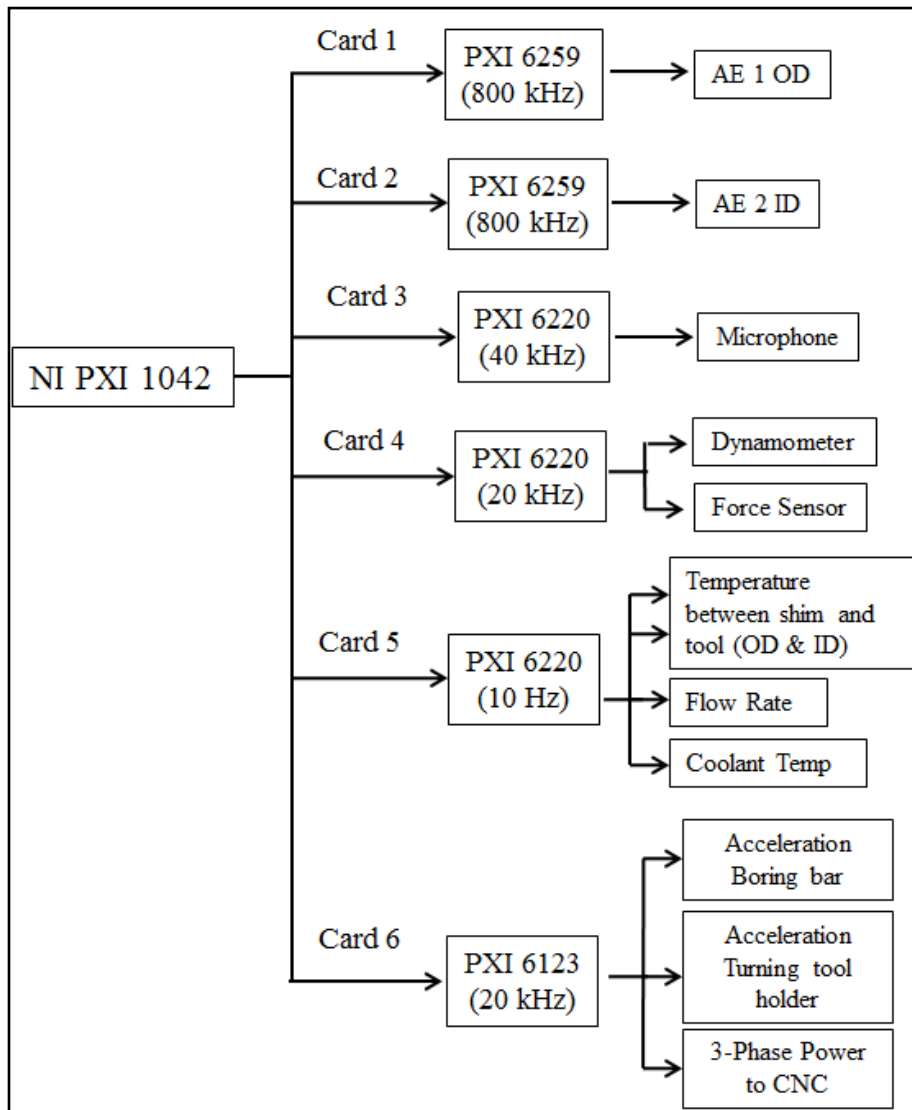


Figure 10: DAQ Setup Diagram

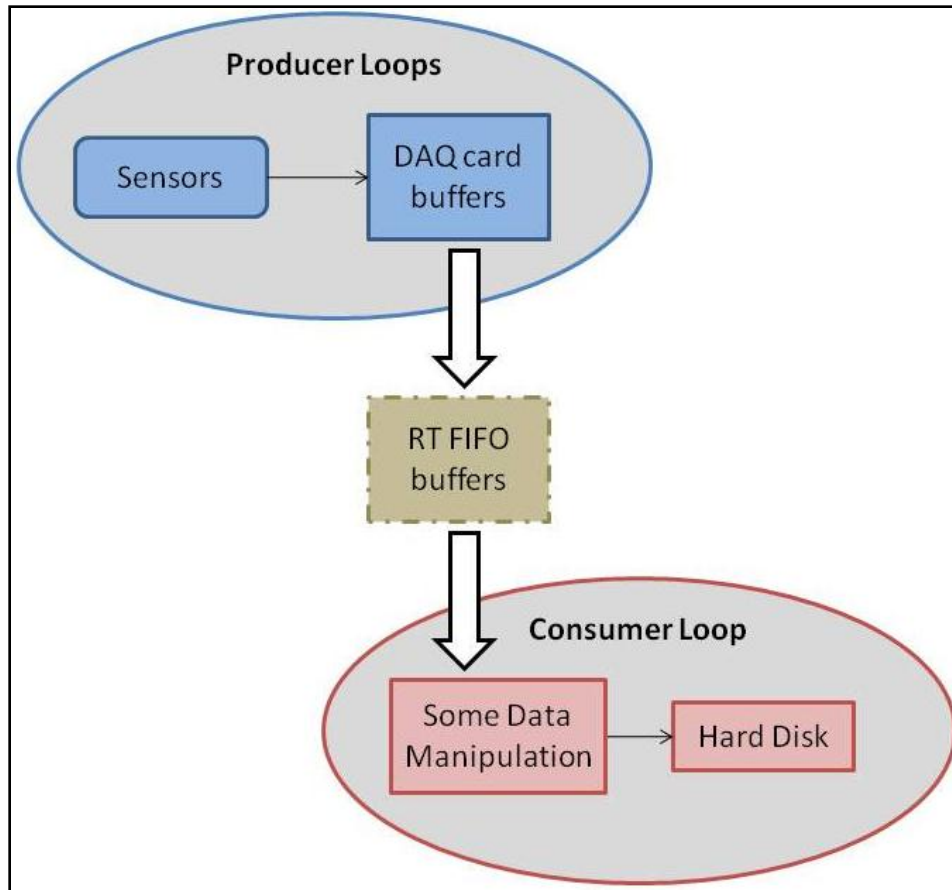


Figure 11: Flow Chart of Data through the Producer-Consumer Architecture

Sensor Information

A Kistler 9121 tool holder dynamometer is installed to correlate the cutting forces at different machine parameters to other factors such as tool condition, chatter, and responses of the power meter and microphone. An adapter made of 1018 steel, shown in figure 12, was designed to fix the dynamometer onto the lower turret. A NI PXI-6220 DAQ card is used to acquire data from the dynamometer at a 20 kHz sampling rate.

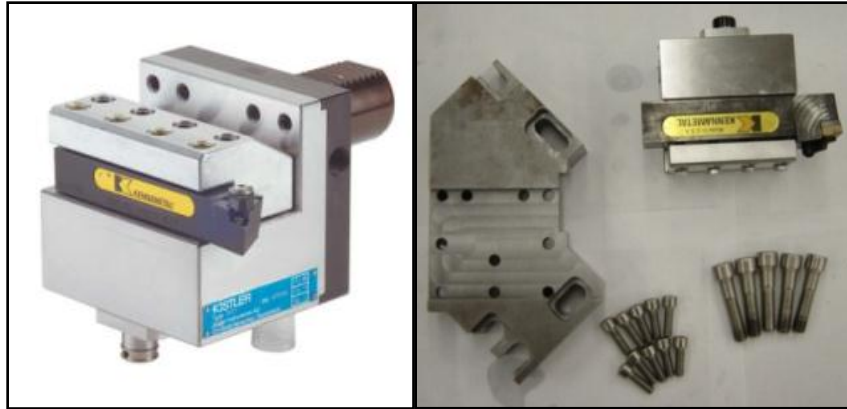


Figure 12: Dynamometer and Adapter Plate

The forces on the inner diameter of the workpiece are detected using four Kistler 9066A4 force sensors, as shown in figure 13. These sensors were used to monitor the cutting forces exerted on the boring bar in three directions (X, Y, and Z) during the machining. Force sensors proved successful in characterizing performance of coated carbide working on AISI 1045[31]. The tangential force response was measured due to the effect of speed, feed and side cutting edge angle. Even the power spectral density response of the feed force is being studied to identify cutting states and chatter[32]. The force sensors were installed between two AISI 1018 steel plates which had grooves machined on them in order to facilitate the mounting of the force sensors. The final assembly of the adapter plates and sensors with the boring bar and turret is shown in figure 14. The force sensors were connected to a set of summing blocks which were subsequently connected to the force amplifier; this amplifier was then connected to a NI PXI 6220 Card being sampled at 20 kHz.

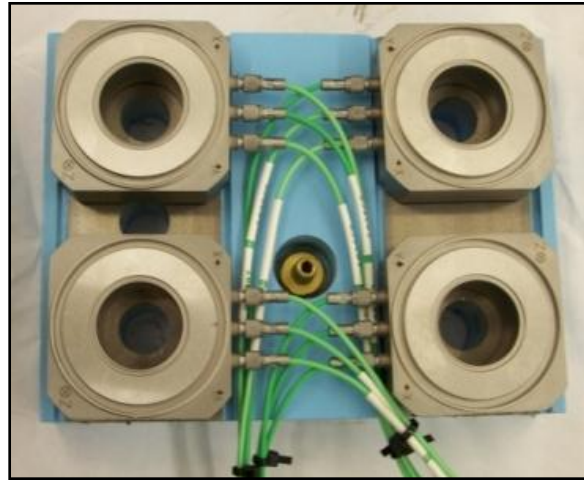


Figure 13: Adapter plate with Force Sensors

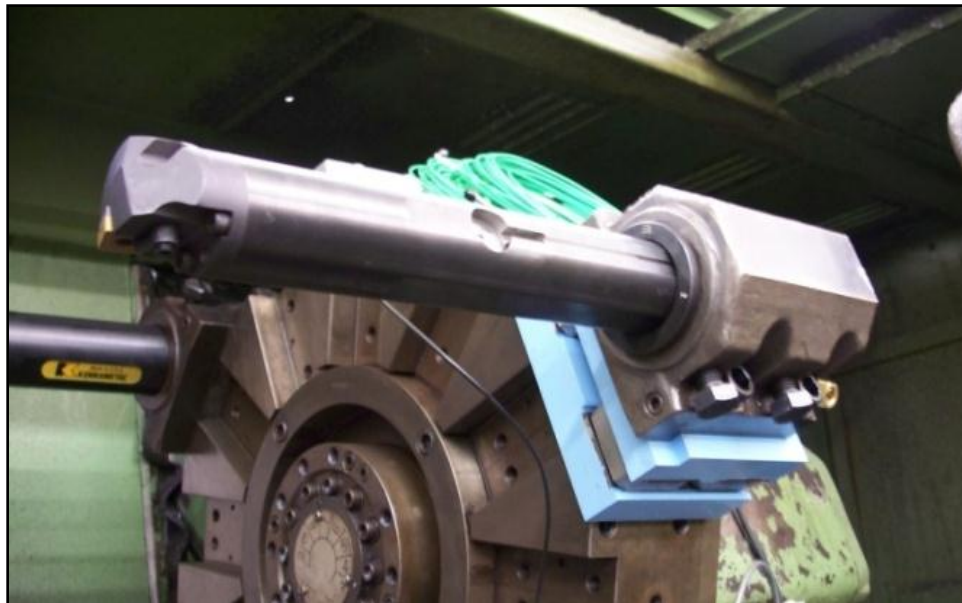


Figure 14: Boring Bar with Adapter Plates and Sensors

Analyzing the tool temperature is important because excessive heat softens the tool and accelerates wear to breakage[33]. From Saglam’s study, temperature can be correlated with the amount of cutting force applied[33]. Omega Engineering K-Type thermocouples were installed

between the tools' insert and shim. In order to install a thermocouple, a groove with a depth and width of 0.5mm was machined into a tool insert holder, as shown in figure 15. Thermally conductive grease was then applied to the groove and the thermocouple was set into location. This location is the most favorable place because it is as close as possible to the tool tip yet clear from machining debris. The thermocouples are connected to a NI SC-2345 signal condition carrier via a NI SCC-TC02 thermocouple signal conditioning module. A NI PXI-6220 DAQ card is used to gather data from the thermocouple at a rate of 10 Hz.



Figure 15: Groove Location for Thermocouple on Insert

A PH-3A Load Controls power meter was installed to measure the power consumption during machining. Transient signals from a power and dynamometer have shown similar trends[34]. The power meter is bolted to the electrical cabinet of the lathe. Cables that connect

the breaker to the rest of the lathe's electromechanical systems are routed through the three toroidal Hall Effect sensors of the meter and then reconnected to the breaker switch using terminal lugs. A NI PXI-6123 acquires data from the power meter at a sampling rate of 20 kHz. Figure 16 shows the power meter, along with a photograph of the installation area.

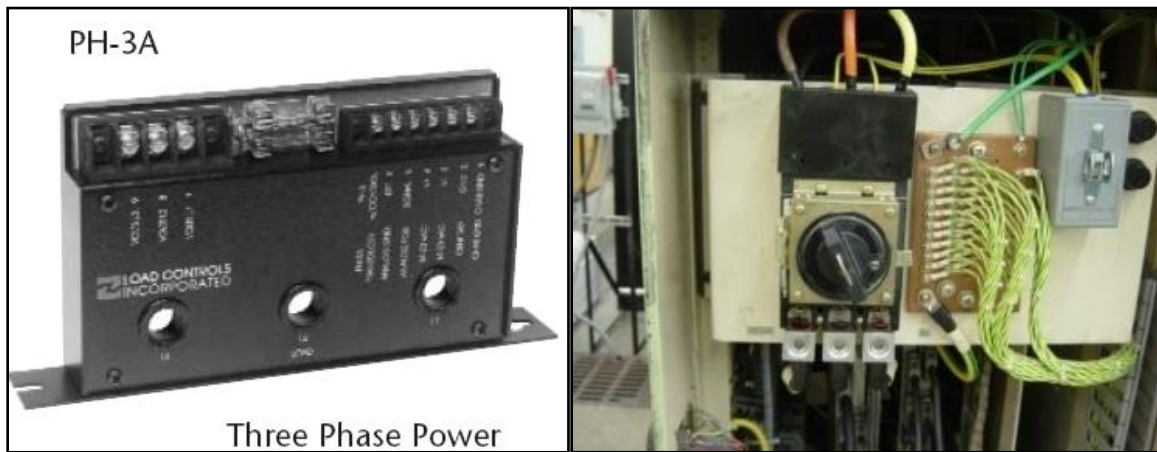


Figure 16: Power Meter in Electrical Cabinet

A Samson Audio Q8 dynamic microphone is used to detect audible sound emitted from the machining process. Correlations can be made between audible sound and tool wear, chatter and tool breakage. The microphone detects audible sound using a neodymium microphone element and the frequency response expected is between 60 Hz and 16k Hz. Research shows that increase in tool wear correlates with an increase in amplitude of the recorded audible noise between 6 Hz and 20k Hz [11]. The microphone is installed through a hole on the top of the turning center (Figure 17). This hole is directly above the workpiece location in order to accurately acquire the audible frequencies emitted during machining. The connection between the microphone and the DAQ is through a NI SCB-68 shielded connector block. A NI PXI-6220

DAQ card samples the microphone at 40k Hz. Analysis of microphone data is performed in the frequency domain to determine how the FFT characteristics of the machining change with time.



Figure 17: Microphone Setup

CHAPTER FOUR: PHASE II DESIGN OF EXPERIMENT

Experimental Design and Evaluation

The experiments for this project were conducted in the Mechanical Engineering Machine Shop at the University of Central Florida. The ambient noise levels in the room were uncontrollable which helped simulate the noisy conditions present in industrial settings. The machining operation involved simultaneous OD turning and ID boring. A new tool edge was used for each experiment to help eliminate variability of tests due to tool wear. After a pass was finished, the hardness, surface roughness, tool condition, and chip color and formation were recorded as post test data.

The data from all sensors was analyzed offline and sensor metrics were extracted. The statistics were computed in the region of data where cutting had taken place. A Labview program analyzed the power meter for indication of steady state machining. When the program identified points of where machining took place it stored statistics of every signal in a comma separated variable format. The columned table of run statistic data was placed into Minitab worksheet for ANOVA analysis and regression.

The wall thickness between the outer diameter and inner diameter of each workpiece was measured radially before every test to observe the effects of eccentricity. A qualitative value about the amount of rust was also gauged. The surface roughness and hardness measurements of the workpieces can be correlated to different sensor signals after analysis. Hardness measurements, using a Leeb hardness tester, were also conducted after each test on the clean OD

portion of the workpiece. Hardness of the workpieces can vary due to the fact that they are forged and stacked to cool in an unknown location and orientation.

The DoE for this set of experiments was a response surface study with a Face Centered Design of four factors, each at two levels. The response surface model contains $2^k + 2k + n_c$ amount of runs, where k is the number of factors and n_c are the centerpoint runs. The factors being feed rate, spindle speed, OD depth of cut and ID depth of cut. Six center points were added to the DoE in order to complete a check for the different curvature of the DoE. Since the goal is to improve factory's current machine settings, they were set as center point values. Single point metrics were taken for each sensor signal from the beginning to the completion of each test. The different metrics used for characterizing the different signals were mean, standard deviation, and the sum. Figure 18 shows the design space for the four factor experimental study. There are two cubes representing the lower level of DOC ID and high level DOC ID. The cube has an axis for each of the remaining factors. The design space also has axial points on each face of the cubes.

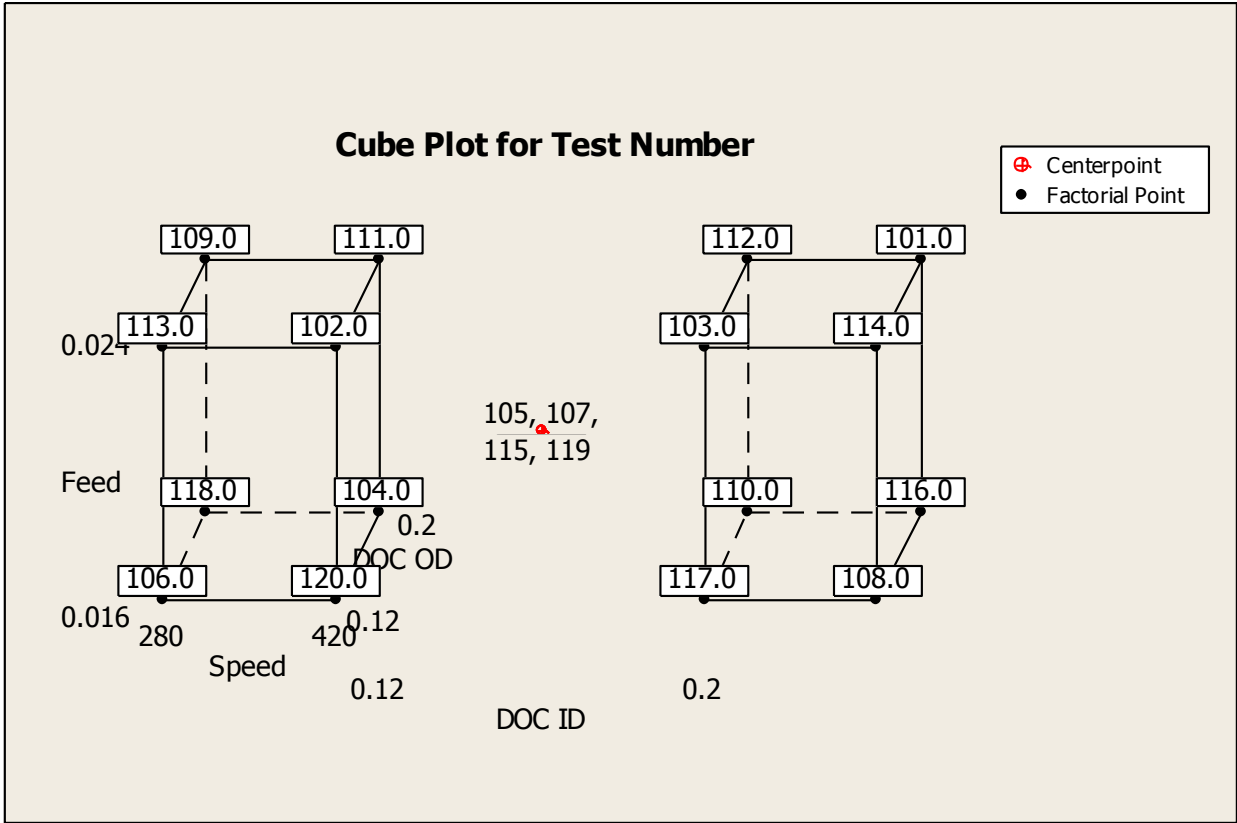


Figure 18: DoE Design Space

The settings for the response surface experiment are shown in table 1. The third block of runs contains the axial points which lie on the faces of each cube in the response surface space. The first two blocks may be analyzed independent of the third as a full factorial design. To validate models and gain more data, this response surface experiment is repeated for test 101 to 130. The DAQ program was started before the machining process and continued until the spindle and axis had stopped. After the run data was transferred to the host machine, a separate Labview program was used to analyze the data on the host machine. First, the program analyzed the power to determine when the operation was in steady state cutting so that the only portion of analysis

took place during the cutting operation. Then, the Labview program on the host computer extracted statistics from every signal in each run offline.

Table 1: Response Surface II Experiments for Simultaneous OD Turning and ID Boring

Test	Pt. Type	Block	Speed (RPM)	Feedrate (in./rev.)	DOC OD (in.)	DOC ID (in.)
131	1	4	280	0.016	0.120	0.200
132	1	4	420	0.016	0.200	0.200
133	1	4	280	0.016	0.200	0.120
134	1	4	420	0.024	0.200	0.120
135	0	4	350	0.020	0.160	0.160
136	1	4	280	0.024	0.200	0.200
137	0	4	350	0.020	0.160	0.160
138	1	4	420	0.016	0.120	0.120
139	1	4	280	0.024	0.120	0.120
140	1	4	420	0.024	0.120	0.200
141	1	5	420	0.024	0.200	0.200
142	0	5	350	0.020	0.160	0.160
143	1	5	420	0.016	0.200	0.120
144	1	5	280	0.016	0.120	0.120
145	1	5	280	0.016	0.200	0.200
146	1	5	280	0.024	0.200	0.120
147	1	5	420	0.024	0.120	0.120
148	0	5	350	0.020	0.160	0.160
149	1	5	280	0.024	0.120	0.200
150	1	5	420	0.016	0.120	0.200
151	-1	6	350	0.020	0.160	0.200
152	-1	6	350	0.020	0.200	0.160
153	-1	6	350	0.016	0.160	0.160
154	0	6	350	0.020	0.160	0.160
155	-1	6	420	0.020	0.160	0.160
156	-1	6	350	0.024	0.160	0.160
157	-1	6	350	0.020	0.120	0.160
158	0	6	350	0.020	0.160	0.160
159	-1	6	350	0.020	0.160	0.120
160	-1	6	280	0.020	0.160	0.160
161	0	6	350	0.020	0.160	0.160

Analyzing DoE response data in Minitab to develop an adequate model is an iterative process. The flow chart in figure 19 illustrates the steps of the process when analyzing a single response. Data in Minitab is organized in a fashion similar to an excel worksheet as in Table 1, with additional columns to the right listing the statistical metric values of different responses.

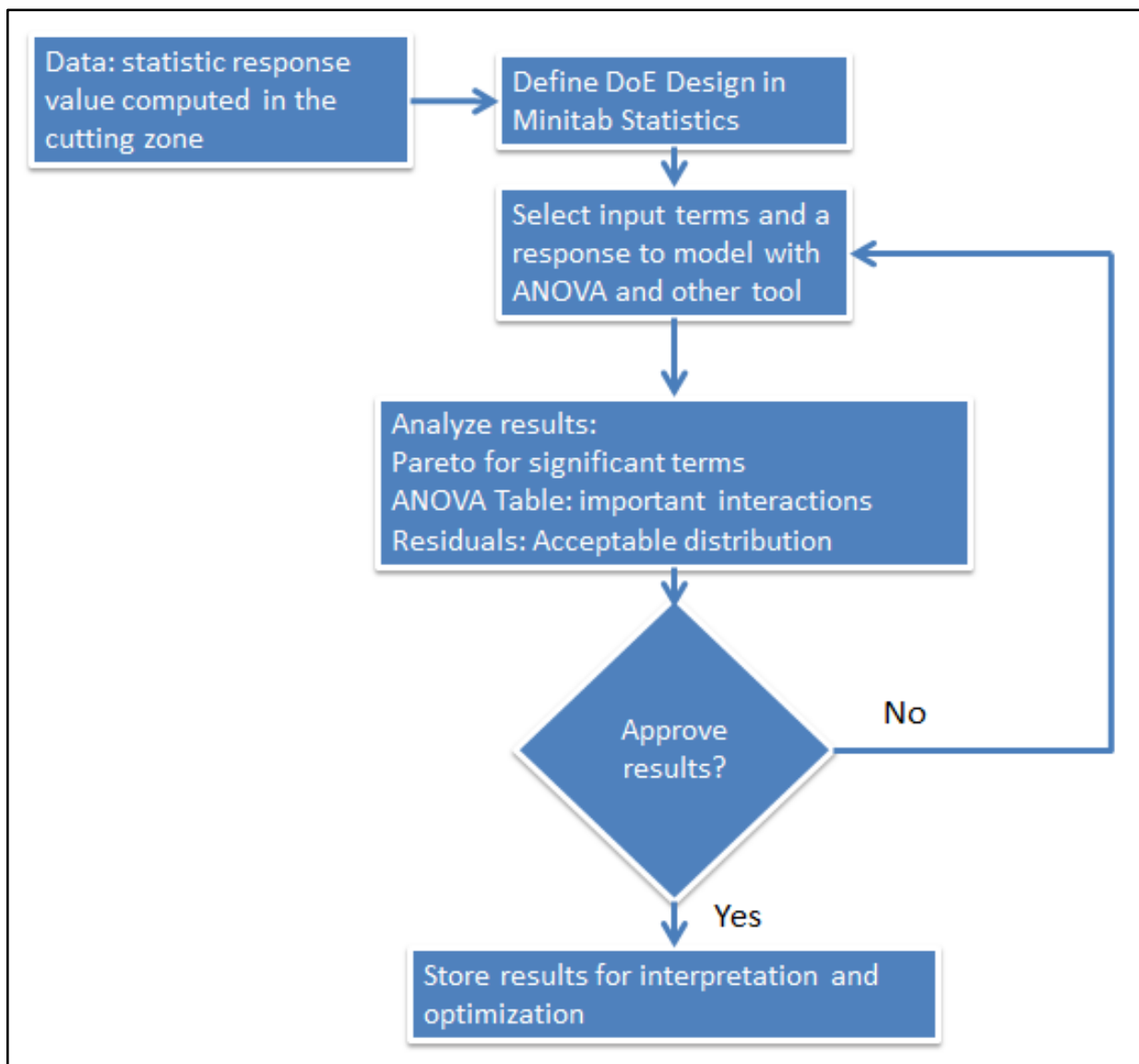


Figure 19: DoE Analysis and Model Fitting

In order to perform the ANOVA in Minitab the study needs to be defined. To define the experiment, Minitab must be set to recognize the column of settings for all input factors, point type column, and block column. Response columns data may contain information such as average power. Each cell in the column is the average power from a combination run. The data has been defined in Minitab Statistics and plots such as the Main Effects for Average Power may be created. The main effects plot is one graphical method to assess the significance of factors on the Average Power response. Analyzing the main effects of average power shows that the value changes by more than 2000 watts for different level of every factor.

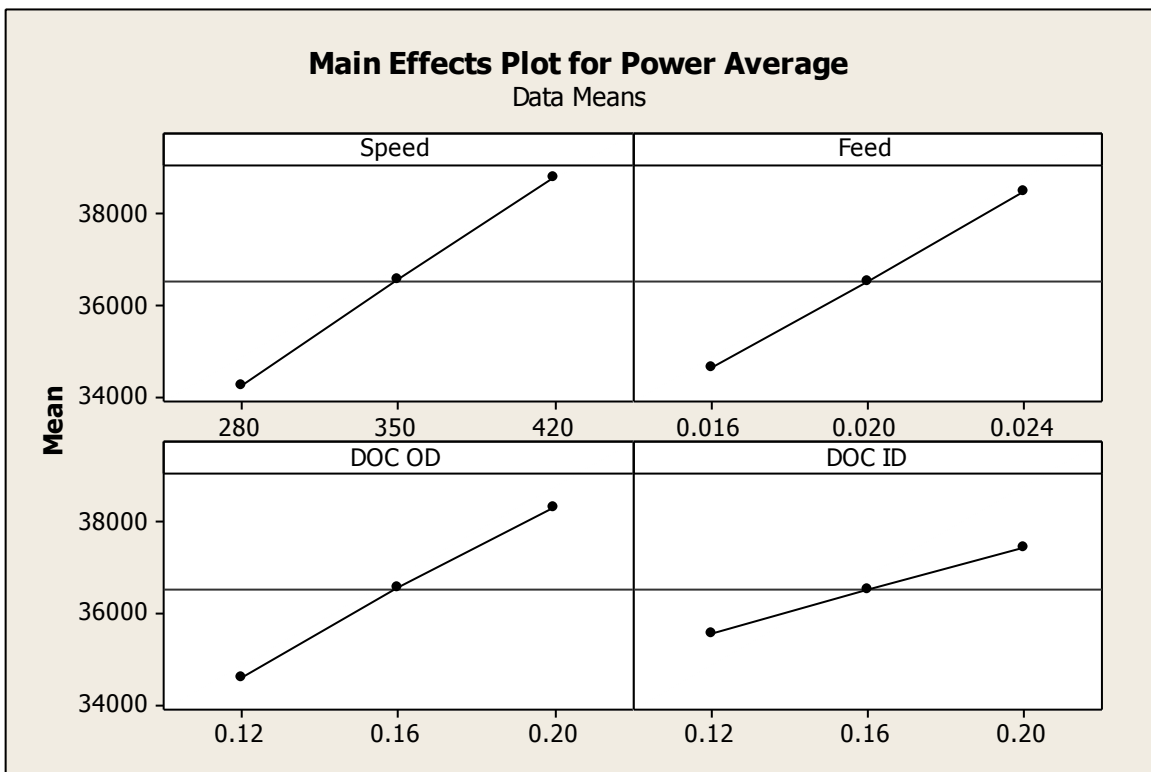


Figure 20: Main Effects Plot of Average Power

To better understand how interaction effects may influence the Average Power response, an ANOVA study is done on the factors and their interactions. Minitab performs the statistical equations required for hypothesis testing and presents the results in the ANOVA table. A linear least square regression with every factor was conducted. The coefficient values and their significance are also included in the results table.

Table 2: Minitab ANOVA Analysis Table for Average Power

Type	Source	P value
Main Effect	Speed	0.00
Main Effect	Feed	0.00
Main Effect	DOC OD	0.00
Main Effect	DOC ID	0.00
2-Way Interaction	Speed*Feed	0.00
2-Way Interaction	Speed*DOC OD	0.00
2-Way Interaction	Feed*DOC OD	0.00
2-Way Interaction	DOC OD*DOC ID	0.44
3-Way Interaction	Speed*Feed*DOC OD	0.79
4-Way Interaction	Speed*Feed*DOC OD*DOC ID	0.79
Error	Curvature	0.33

The table presents results for the investigator to interpret how well the factors and their interactions predict the average power of the CNC machine. The task is to analyze different pieces of the table and decide if some predictors should be eliminated from the regression. The R squared of the regression with every factor and interaction is over 90%. There may be unnecessary terms in the equation. If the P value is less than 0.05, it is considered significant. All four and three way interaction terms do not increase the accuracy for the estimation of average power. Since the interaction term, DOCID*DOCOD, has a P value of 0.4 it is also not regarded as significant. The effect of curvature is also assessed by a P value in the ANOVA table. The P

value for curvature is greater than 0.3, implying that the average power does not exhibit second order effects from the process in the experiment range.

Another iteration of analysis with updated significant terms is performed on the Average Power response. A Pareto chart of the average power response can visualize the significance of all terms in the analysis by representing the standardized effects of each factor. The red line is a cut off limit for significant effects.

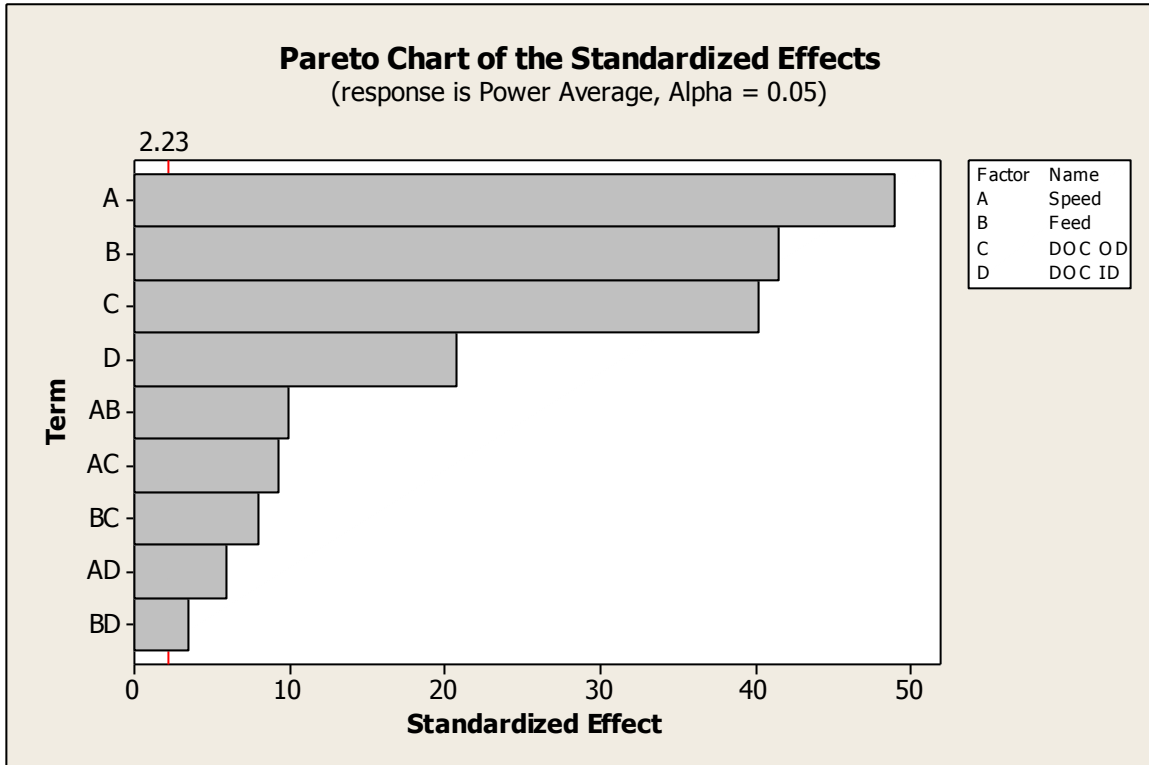


Figure 21: Pareto Chart of the Significant Effects for Average Power

The second iteration of average power analysis with reduced terms improved results. The average power regression equation with fewer terms has a predicted R squared of 99%.

Table 3: Estimated Regression of Average Power with Updated Terms

Term	Coefficient	P
Constant	21649.2	0.00
Speed	15.3539	0.00
Feed	54100	0.00
DOC OD	19021.0	0.00
DOC ID	25503.8	0.00
Speed*Feed	-453.13	0.00
Speed*DOC OD	-66.553	0.00
Feed*DOC OD	344061	0.00
Feed*DOC ID	-161583	0.091

Analyzing the residuals will determine how good the model fits the regression and ANOVA. The normal probability subplot of residuals shows that the residuals from the runs are normally distributed because the residuals are near the blue line. Normal distribution is necessary to produce unbiased estimation from the least squares method. The histogram of residual for average power also shows that the distribution displays a normal trend without any skewedness.

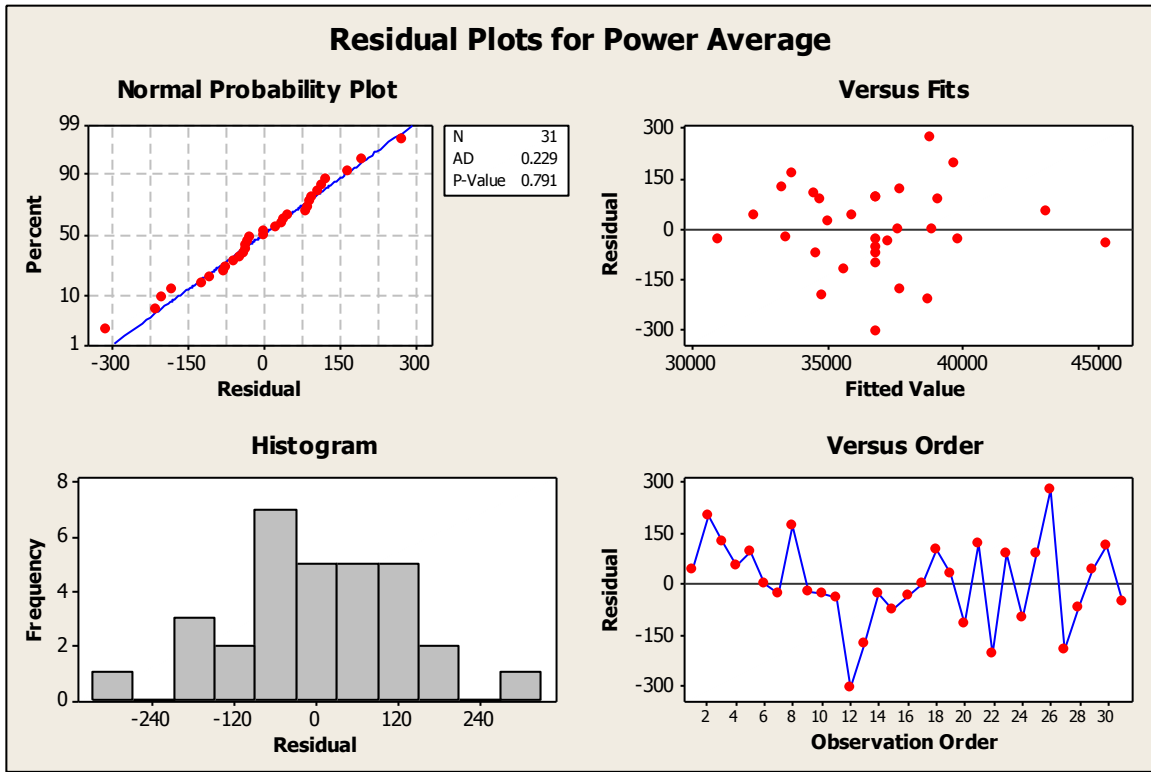


Figure 22: Plot of Residual Results for Final ANOVA Regression

The exact spindle speed, feedrate, OD DOC and ID DOC terms of the RS II regression analysis were included in the RS III analysis which resulted in an R^2 value of 99% for both sets of experiments. The derived response surface models are capable of predicting the average power within plus or minus 250 watts. Keep in mind the underlying difference between RSII and RSIII was that in RSIII there was no cleaning pass to remove rust. The models indicate that the tool is in its early stages of wear. From the tool life studies conducted, we have learned that the average power follows a similar increasing trend with increasing wear. Therefore as the wear increases, the error in our model will also increase. Tracking the trend in error with increasing average

power due to wear may prove advantageous in developing a multisensory wear detection mechanism.

Table 4: Comparison of Regression Equation to RS III

Test	Speed	Feed	DOC OD	DOC ID	RSIII Avg. Watts	Predicted	Difference
162	280	0.016	0.120	0.120	31091.8	30988.5	-103.3
163	420	0.024	0.120	0.120	37649.6	37636.0	-13.6
164	350	0.020	0.160	0.160	36568.4	36786.2	217.8
165	280	0.016	0.200	0.200	34752.1	34624.9	-127.2
166	280	0.024	0.120	0.200	34955.7	35059.4	103.7
167	350	0.020	0.160	0.160	36687.3	36786.2	98.9
168	420	0.016	0.200	0.120	37938.8	37719.2	-219.6
169	280	0.024	0.200	0.120	36981.9	37276.4	294.5
170	420	0.016	0.120	0.200	35968.5	35657.1	-311.4
171	420	0.024	0.200	0.200	45284.6	45328.6	44.0
172	350	0.020	0.160	0.160	37051.5	36786.2	-265.3
173	280	0.016	0.120	0.200	31878.7	32286.9	408.2
174	280	0.024	0.200	0.200	38839.9	38842.7	2.8
175	420	0.016	0.120	0.120	33934.1	33698.4	-235.7
176	280	0.024	0.120	0.120	33403.3	33493.1	89.8
177	420	0.024	0.200	0.120	42972.8	43102.1	129.3
178	420	0.016	0.200	0.200	39711.9	39677.9	-34.0
179	280	0.016	0.200	0.120	33572.6	33326.4	-246.2
180	350	0.020	0.160	0.160	36918.2	36786.2	-132.0
181	420	0.024	0.120	0.200	39859.6	39862.5	2.9
182	350	0.020	0.160	0.160	37063.7	36786.2	-277.5
999	380	0.022	0.160	0.160	39066.71	38867.7	-199.0

All sensor responses have been analyzed according to the DoE analysis model presented. Table 5 lists some turning and boring sensor responses along with their primary factors with Y highlighted. The feed force was a significant factor for every response in Table 5. Also, the associated depth of cut was a primary factor between the OD and ID average temperature near

the tool response. The ID and OD feed force is affected by the feedrate and depth of cut. It was unusual to observe that the tangential turning force is also affected by the feedrate for the range of settings.

The average surface roughness was only a factor of the feedrate. As long as the tool is completely embedded in the material, the surface finish is acceptable in all extreme ends of the design space. If the depth of cut is low and the workpiece eccentricity is great, there is a chance that the tool may not fully embed in the material.

Table 5: Main Effects of Other Response Averages

OD Sensor	Speed	Feed	DOC	SxF	FxDOCOD
Average OD Tool Temp	N	Y	Y	N	N
Average Turning Force (Fz)	N	Y	Y	N	Y
Average Feed Force (Fy)	N	Y	Y	N	N
Average Surface Roughness	N	Y	N	N	N
Average Power	Y	Y	Y	Y	Y
Average ID Tool Temp	N	Y	Y	N	N
Average Feed Force (Fx)	N	Y	Y	N	Y
Average Tangential. Force (Fy)	N	Y	Y	N	N

Tool Life Study

The tool life experiments are a major contribution to the overall cost optimization and are also fundamental methods for characterizing equations necessary in any monitoring system. A Taylor Tool Life model was derived from runs in a DoE. Several publications have been made in fitting a TTL model with DoE. The equation is linear when it is in the natural logarithm form. The factors of the TTL model are cutting speed and feedrate with response time in minutes. The

cutting speed is a function of the RPM and radial location of the tool edge. Essentially, the cutting speed is the tangential velocity between the tool and workpiece.

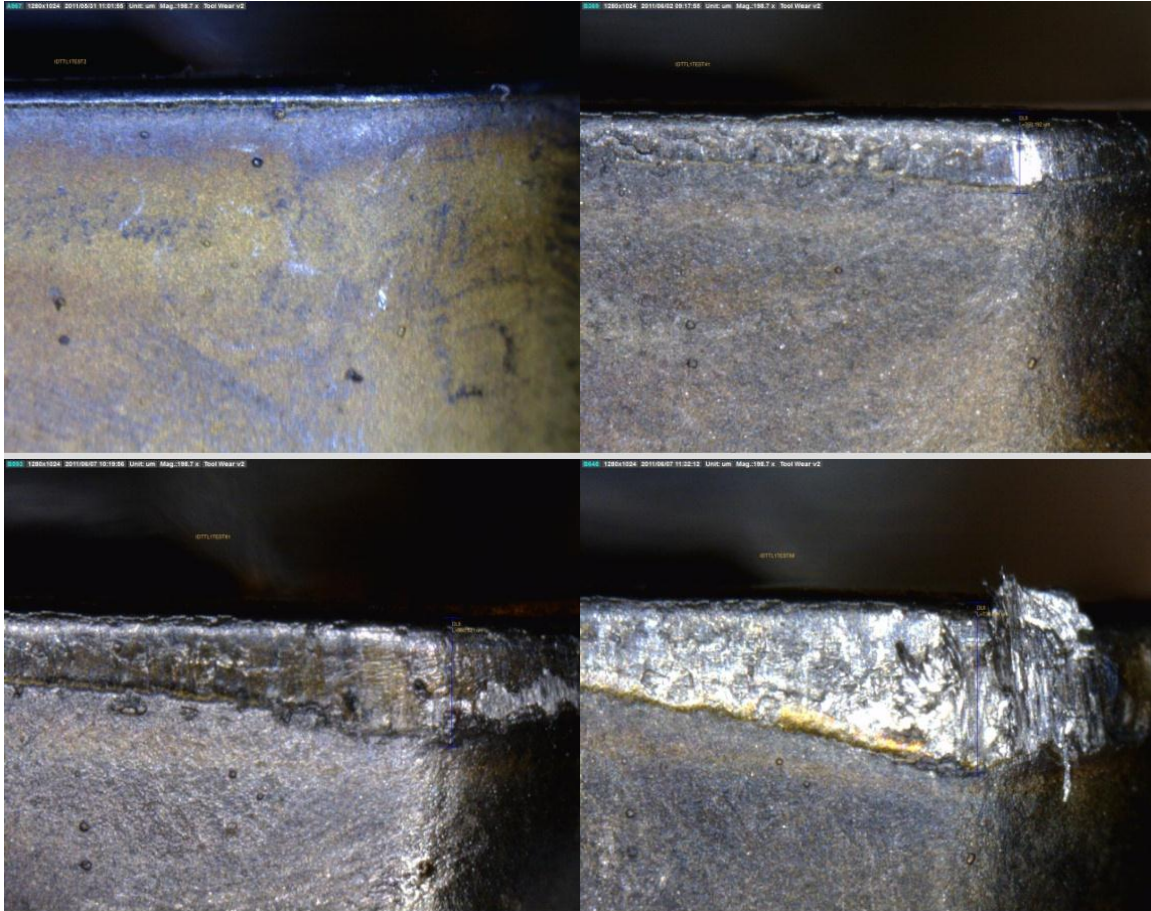


Figure 23: Turning Tool Wear Microscope Pictures for pass #1, #7, #14, #19

The cutting speed and feed rate settings for the experiment runs are in Table 6. Cutting speed and feedrate each have two levels for a two-squared factorial experiment. Runs 5 and 6 are repeats to validate the model. The depth of cut was held constant at 0.160 inches. In each run, the tool underwent several operation passes until the tool was severely worn. After each pass, a microscope was used to measure the amount of flank wear from one pass to the next. The limit

before the tool is considered severely worn is 500 micron. After the flank wear measured greater than 500 micron, the run was complete. The sum of time for all of the operation passes is the response for each experiment run.

$$T(\text{minutes}) = 2.51023 * 10^{10} * v^{-4.625846} * f^{-3.816334} \quad (3)$$

Table 6: Experiment Runs

Run	Cutting Speed (m/min)	Feed (mm/rev)	DOE Tool Life (min)	Taylor Tool Life Fits (min)
1	219.688	0.6096	2.2002	2.4390
2	219.688	0.5080	5.5337	4.8910
3	183.073	0.6096	6.4147	5.6689
4	183.073	0.5080	11.197	11.368
5	183.073	0.5080	10.198	11.368
6	219.688	0.6096	2.3893	2.4390

The derived tool life model is a good fit for the data within the design space. The derived constants were used to estimate the ID tool life. For ID tools, the tool life is extended because the ID surface speed is much lower for the standard 350 RPM. Only two runs were performed first at high surface speed and feedrate, then at nominal surface speed and feedrate. Though there were not enough runs to derive three constants for only ID tools, Table 7 shows that model for OD tooling is adequate. When using the constants derived from the OD turning tool runs, the percent error was less than seven percent. This shows that the constants relate more to the property to the tool material.

Table 7: ID Prediction Results

Test	Predicted (min)	Experiment (min)	% Error
1	43	46	6.98
2	1634	1545	-5.45

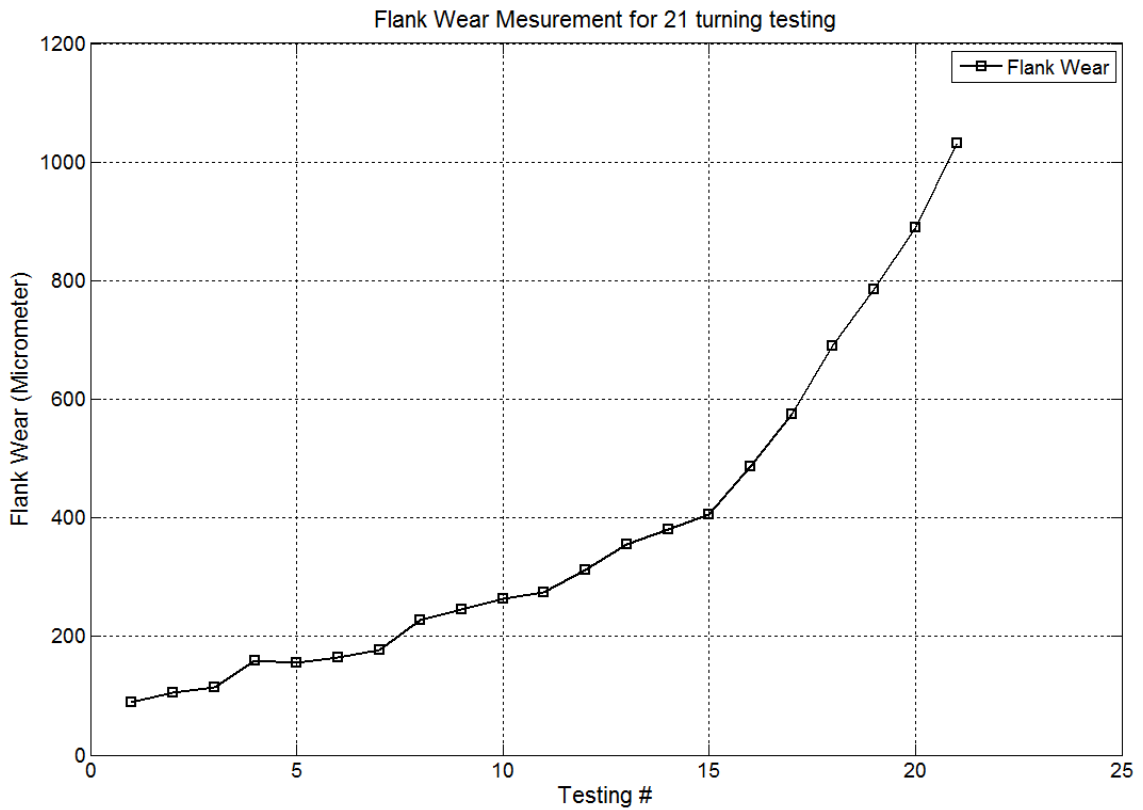


Figure 24: Flank Wear versus Tool Pass Number

Whether the flank wear is a function of time or operation number, the trend shows a linear stage in early tool wear followed by larger increases after the wear has passed 500microns. As the wear increases, the average force exerted on the tool after each operation pass follows a similar trend. The same general sensor trends in the time domain were seen in the recent tests as

the previous tool wear tests. The dynamometer data provided information of the forces that were exerted near failure. The feed forces for all failure tests lied in a region very close to 5 kN for a set of different machining settings. This is important when determining a control model because when a force over 4.5 kN is recorded, the machine can let the operator know it is time to change the tool. The average power also shows a significant relation to the flank wear trend. It is apparent that the power meter may be implanted as one of the methods to aid in detecting imminent tool failure.

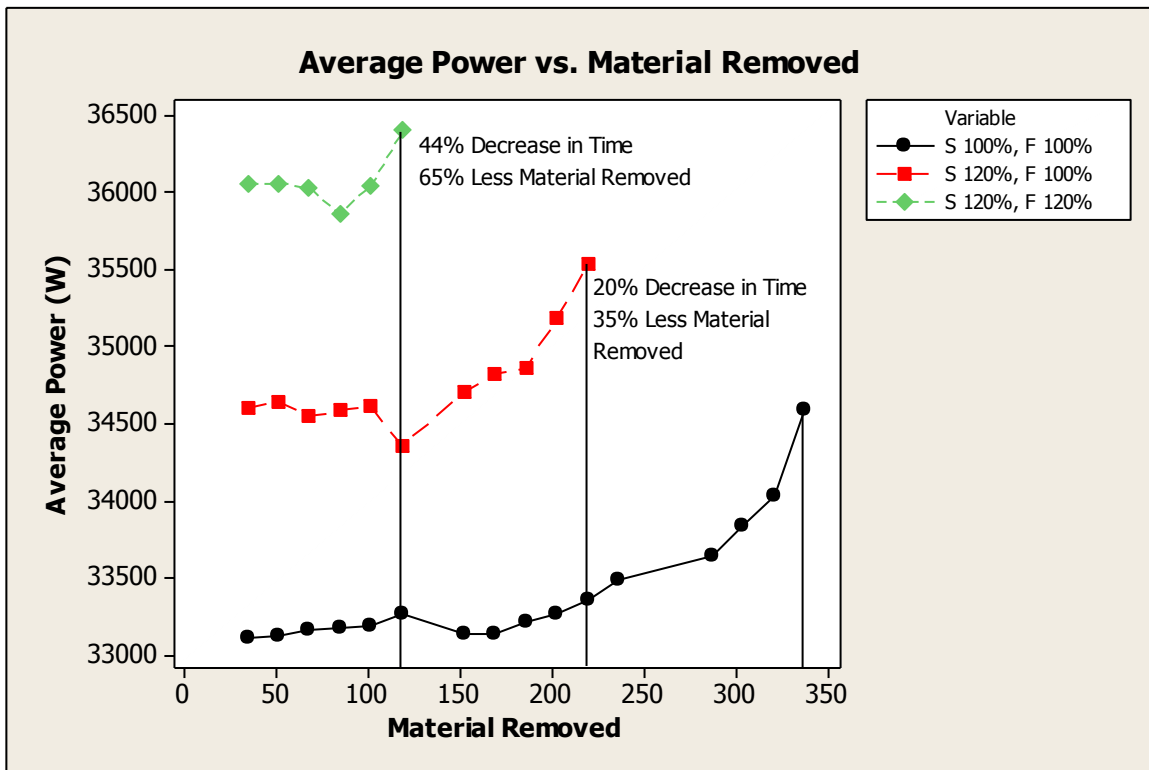


Figure 25: Power at Different Factors versus Material Removed

Figure 25 shows the average power as a function of material removed from different tool wear tests. The black line plots average power results from a test conducted at the Factory

settings. The red line settings are 120% above Factory's normal spindle speed and the feedrate is equivalent to their 0.020 inches per revolution. From looking at each response, it is apparent that as the settings increase, the tool life decreases, along with the change in power from the beginning of the tool life to the end. Thus, at the Factory (black line) and red line settings, it is possible estimate the failure as the tool approaches 0.5 mm of wear. Since the proposed optimal settings set both the feed and speed 110% above the factory settings, the hypothesis is that the most favorable power signal trend will lie between the red and black lines.

The conditions proposed for the research did not suggest the wear to be an issue since the roughing operations from RS II and RS III had acceptable finishes for a successful finishing pass. A scatter plot of average roughness shows there is no notable trend like that seen in the forces, power, or temperature data. As long as the tool does not fail during a cutting operation, there is no concern regarding proper surface finish for the proposed range of optimal conditions

Frequency domain results from the tool life experiments provide great insight into wear trends that will be used to develop a monitoring system. Waterfall plots were developed to show how the frequency of the signals change over the flank wear trend. Figures 26 include only tests that involved rust removal thus emulating factory conditions. There is an apparent microphone frequency shift from 8750 Hz to 8150 Hz as the tool wear passes the linear wear region (0 - 0.50 mm) and enters the exponential wear region (0.50 mm - failure). The power meter's PSD frequency also followed a similar pattern of shifting frequencies.

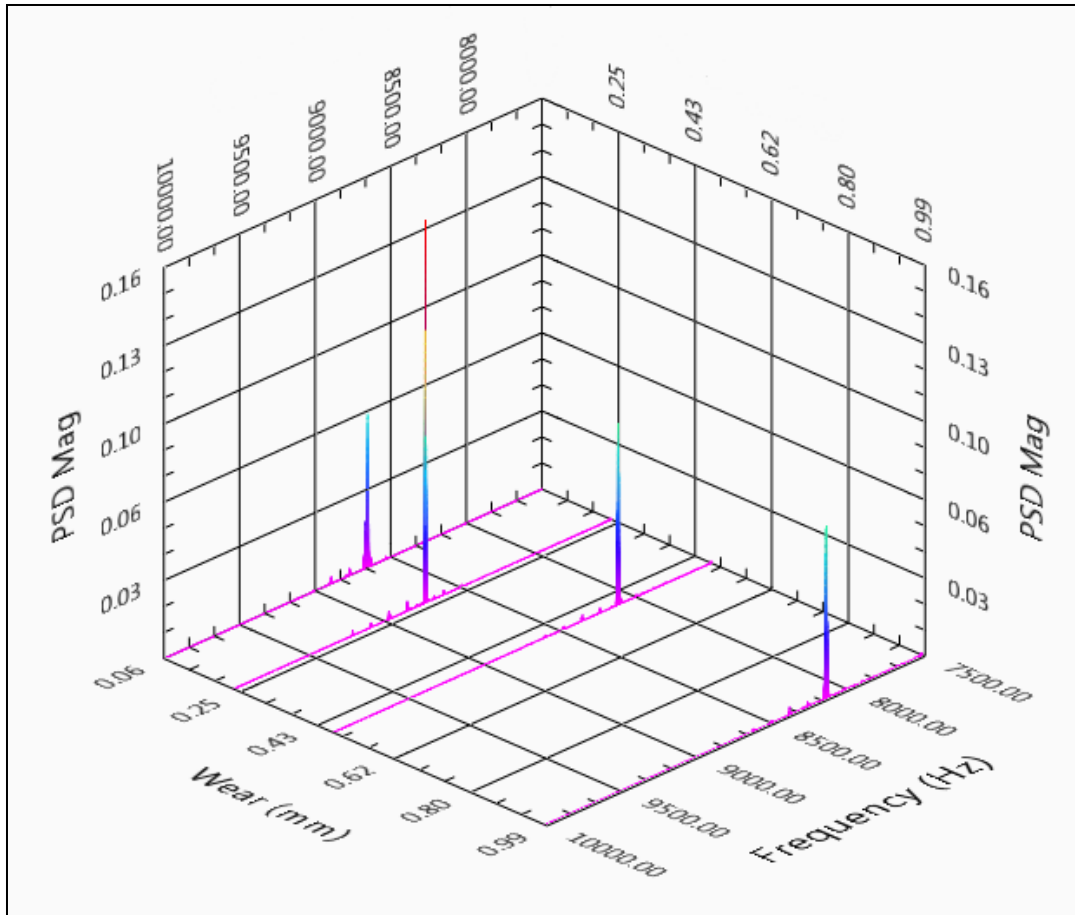


Figure 26: Waterfall plot of Microphone PSD at Factory Settings

As a fresh tool's wear progresses in the linear region, the frequency remains constant and the amplitude increases. When the tool enters the exponential wear region (> 0.5 mm), the frequency shifts to 8150 Hz. The same exact trend is recognizable across the frequency response of the dynamometer's X and Y axes. The results realize the potential for the microphone and power meter to be used in a robust adaptive control system with reduced sensors.

A literature review of similar studies proved that the root mean square (RMS) of acoustic emissions (AE) is useful in determining tool wear states. Waterfall plots can show the RMS

signal trend with respect to tool wear. As the tool approaches failure the variation in the RMS signal notably increases.

The goal of the project is to develop a system to continuously optimize cost and tool life. The tool life study benefited the development of a tool life model as function of surface speed and feedrate. The estimation of tool life aids the understanding of machining cost, and the analysis of tool wear experiment also provided insight to methods of detecting tool wear.

CHAPTER FIVE: OPTIMIZATION AND VALIDATION DISCUSSION

The focus of the thesis has been the selection of settings through DoE to reduce machining cost. The machining cost function (2) consists of direct energy cost, tool cost, and labor cost. The DoE studies for energy consumption and tool life were beneficial in developing a model of equation. This portion of the paper aims to optimize the cost function as a function of spindle RPM and feedrate. Then, the results will be validated when the optimized settings are run and compared to predicted values.

The energy cost is the first portion of the equation and is computed from the average power, time of machining and rate of energy in \$/kW hr. In a real time monitoring application, the average power may be estimated from the DoE regression model or measured directly from the power meter. The tool cost part of the cost function depends on the cost of the tool edge, time of machining, and TTL equation. The TTL equation is dependent on the surface cutting speed and feedrate. As mentioned, the surface cutting speed represents the tangential velocity between the tool and workpiece. The radial location of the tool is dependent upon the workpiece dimension and depth of cut and the time of machining in minutes is computed by the length of the cut divided by the product of the RPM and feedrate.

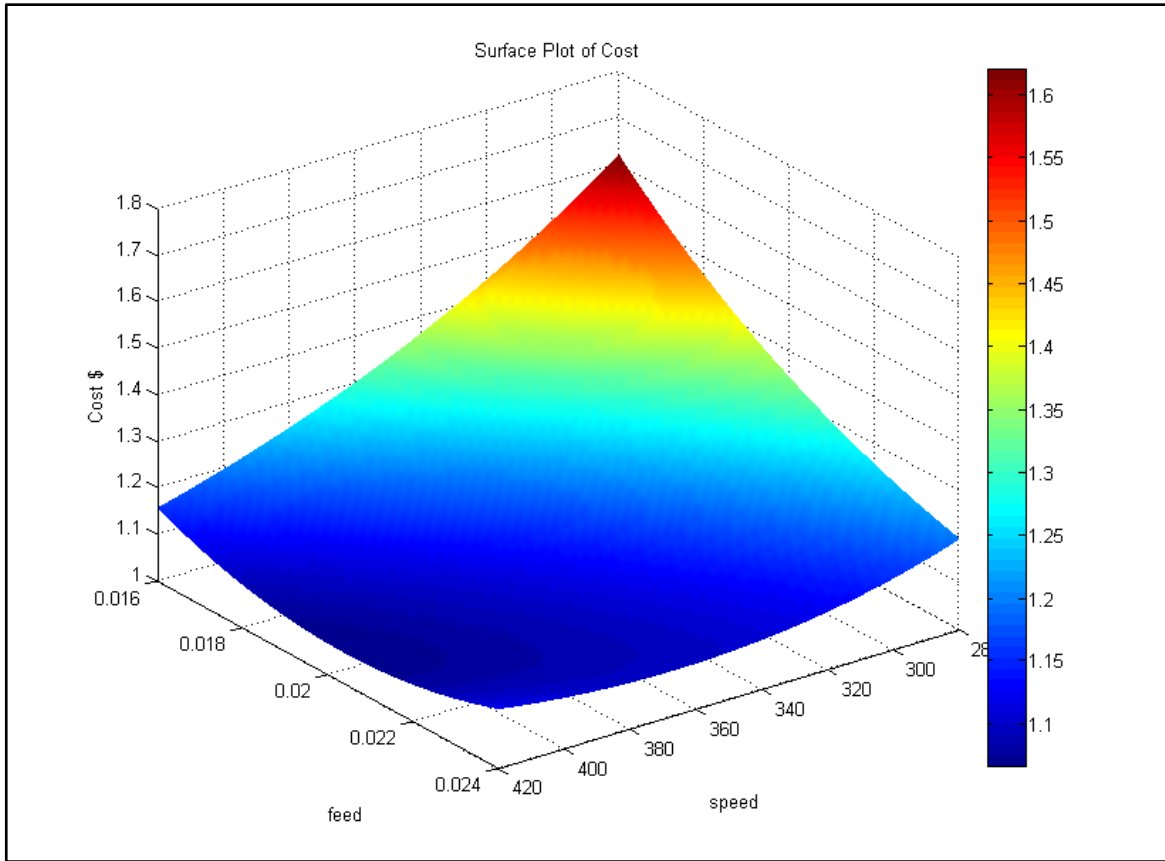


Figure 27: Surface Plot of Tool Cost

Considering the constants specific to the factory, like cost per tool edge, machinist labor rate, and energy cost, the cost at current settings of 350RPM and 0.020 IPR is \$1.15. The cost function is nonlinear and shows an area of lower cost with greater RPM and feedrate. It is useful for the cost function to be dependent on RPM and feedrate since the CNC panel has mechanical override switches for spindle speed percent and feedrate percent. The cost function minimum occurs at 380 RPM and feedrate near 0.022 IPR and shows a value of \$1.08.

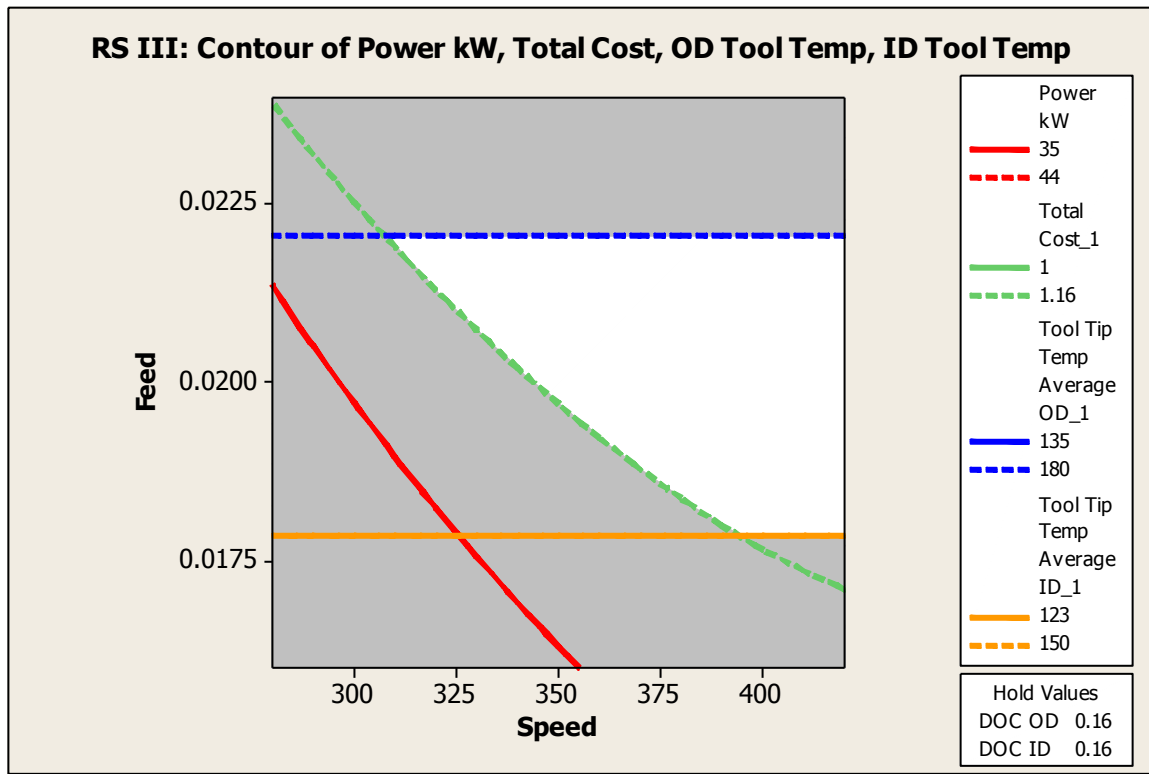


Figure 28: Overlaid Contour Plot of Cost and Other Responses

An overlaid contour plot of specific sensor responses helps to visualize a boundary of compromise over a range of machining parameters. In Figure 29, the response surface III regression models of average power, total cost, OD tool temperature and ID tool temperature are optimized to reduce the average power and tool temperature. The average power is limited to 44kW since the machine’s maximum HP is 60. The green trend line is the minimal acceptable cost of machining set by the factory’s current cost of machining at \$1.15. By machining at speeds greater than 350 RPM and feedrate greater than 0.020 IPR, a lower cost than the current settings may be achieved. For any settings which fall in the white region, conditions are met so

that the responses are better than at factory settings. To develop an overlaid contour plot, the speed and feed factors were varied while the depths of cuts were held constant at 0.160 inch.

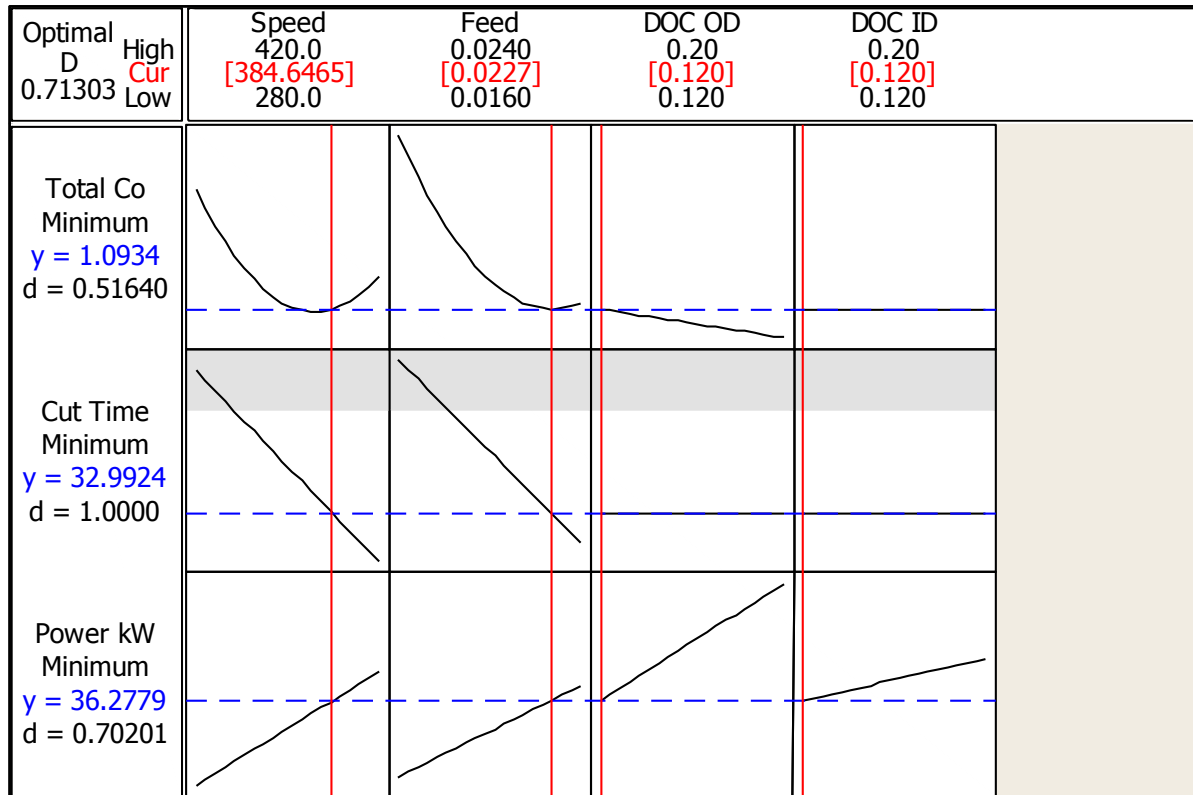


Figure 29: Optimal Settings from Response Optimizer

Any number of regression model responses can be included into a response optimizer. Minitab's response optimizer will identify a combination of input settings which optimize a set of responses. The total cost, cut time and average power were the responses of interest to determine global optimal settings. It was desired to minimize the cut time lower than the time to machine at the nominal 350 RPM and 0.020 IPR as well as to minimize the average power and cost as much as possible. According to the numerical optimization in Minitab, the settings which will minimize all of the responses are 385 RPM and 0.022 IPR with low depths of cut. At the

proposed optimal settings, the cost will be reduced to \$1.09 per machining pass and the average power is still significantly less than the machines limit.

Table 8: Comparison of Results to

Factors	Validation Run	Predicted	Results at Factory Settings	% Savings vs. Factory	% error between predicted
Feedrate (IPR)	0.022	0.022	0.02		
Spindle Speed (RPM)	380	380	350		
OD depth of cut (inch)	0.16	0.16	0.16		
ID depth of cut (inch)	0.16	0.16	0.16		
Initial Outer Diameter	6.875	6.875	6.875		
Initial Bore Diameter	3.125	3.125	3.125		
Response					
Cutting Time (Seconds)	35.6	35.9	42.9	16.9	-0.8
Average Power (Watts)	39066	38867.70	36857.82	-6.0	0.5
Power Consumption (kWh)	0.3863	0.3874	0.4388	12.0	-0.3
OD Tool Temp. (F)	195	183.36	136.00	-43.4	6.3
ID Tool Temp. (F)	126	132.14	123.24	-2.2	-4.6
OD Force (tangential cutting) (N)	4548.82	3291.49	3431.93	-32.5	38.2
OD Feed Force (N)	2397.74	2719.80	2579.12	7.0	-11.8
ID Force (tangential cutting) (N)	3713.50	3603.74	3406.90	-9.0	3.0
IF Feed Force (N)	1711.85	1698.07	1616.82	-5.9	0.8
OD Tool Life (Minutes)	5.40	5.40	11.37	52.5	0.0
ID Tool Life (Minutes)	105.90	105.90	222.88	52.5	0.0
OD Tool Cost	0.220	0.221	0.126	-74.8	-0.8
ID Tool Cost	0.006	0.006	0.003	-74.8	-0.8
Energy Cost	0.031	0.031	0.035	12.0	-0.3
Machinist Cost	0.819	0.825	0.986	16.9	-0.8
Total Cost	1.075	1.083	1.150	6.5	-0.8

An important part of the experiment is validating conclusion of the optimal settings.

Table 8 displays results from validation run compared to predicted values and also values at the

nominal factory settings. The factor settings for the validation run are the optimal settings of 350 RPM and 0.020 IPR with the depth of cut at nominal factory settings.

The depth of cut was set at the nominal value of 0.160 because it is not as easy to control during the cutting process, whereas the spindle speed and feedrate are easily controlled with the mechanical override switches. The override switches allow the machine to change the spindle speed and feedrate during the process. If the machine operator suspects indications of tool wear or chatter, it is normal for him to adjust these override settings during the machining process. The depth of cut at the nominal factory settings also ensures that the part is within the specified limit to perform the finishing pass. If depth of cut was too shallow, the part may need additional machining to bring it into tolerance for the finishing pass on another machine.

The second to last column of Table 8 indicates the percentage of savings for each response when using the optimal settings over the previous factory settings. The reduction of cut time from 42 seconds to 36 seconds, at optimal settings, is significant in the overall cost reduction. The machining cut time is part of the power consumption, tool life and machinist rate. Though the average power at optimal settings is greater than at nominal factory settings, the power consumed has been reduced greatly. The power consumption is a product of the average power for the time it takes to machine. The energy cost is reduced by machining faster at a slightly increased average power. The OD tool cost affects the total cost more than ID tool cost and energy cost. Based on the life of the ID tool, the limiting factor is the cost brought on by the OD tool.

The last column presents the percent error between the measured response value and the predicted value from the regression at the optimal settings. The results from the OD tool temperature followed a similar trend to the OD tangential cutting force, and increasing the settings would increase both responses. As expected, the experimental value was greater than the predicted value for both OD tool temperature and OD cutting force because the RPM was greater. Throughout a single test, the variation in temperature is minimal, always less than 5 degrees, even for high feed and high speed cuts. However, comparing the average temperature from center point to center point reveals a large variation for both ID and OD tool temperature response. Thermocouples are sensitive to environmental changes and have lower response times compared to forces, so conducting the experiment at different times of the year would cause variability in the temperature response. Another thought is that any residual heat due to cutting process timed close together would not let the thermocouple cool down to the same temperature each time.

The regression model for average power is less than one percent of the actual average power value at the optimal settings. The operation cutting time is also predictable to a percent less than one. Also, the experiment to characterize tool life was able to approximate the life in minutes within five percent of the actual value. Considering the constants, which may be different for every plant, the cost function is an accurate representation of actual machining cost. The optimal settings from the DoE data were validated and produced a savings of six percent for the machining cost.

Fusing data from the microphone and power meter will give a better perception to the state of the tool. The microphone and power meter are not intrusive to the machining operation, unlike the dynamometer, the power meter and microphone do not physically alter the geometry of the tooling assembly. If sensors mounted to the tooling have wires that do not allow the turret to rotate for multiple operations, they are not practical for industry. Using a power meter and microphone in a monitoring system is cost effective considering a set of monitoring system for multiple CNC machines.

Phase III of the project will involve the development of a CNC monitoring and control system. The cost of the CNC machining operation will be monitored and optimized during the process and the tool life will also be monitored because it is part of the tool cost. Not to mention the cost saved from fewer tool breakages and re-machining of poor surface finish or scrapped parts. Figure 30 displays a possible function block diagram for the first version of a machine cost and tool monitoring system. Many blocks of the diagram incorporate function of programs used throughout the DoE studies. For the purpose of retro-fitting a factory machine for industrial purpose, it is important to have a user friendly monitoring system.

The DoE analysis provided necessary information to assess the feasibility of various sensors for a monitoring system. National Instruments Labview software and hardware has the capability to develop an industrial CNC monitoring system. The power meter is a great sensor to use for monitoring the state of machining and tool. As the study results suggest, there is trend between increasing wear and average power. The power meter can also be used to monitor the energy cost of the machine. A microphone placed near the cutting zone can provide data to

assess the machining. Features of tool wear can be observed by analyzing the frequency domain of a microphone. The figure conceptualizes the functions necessary to monitor the CNC process. It takes into account usability by having “machine constants” read from G code analyzer and cycling through the multiple operations performed by each turret.

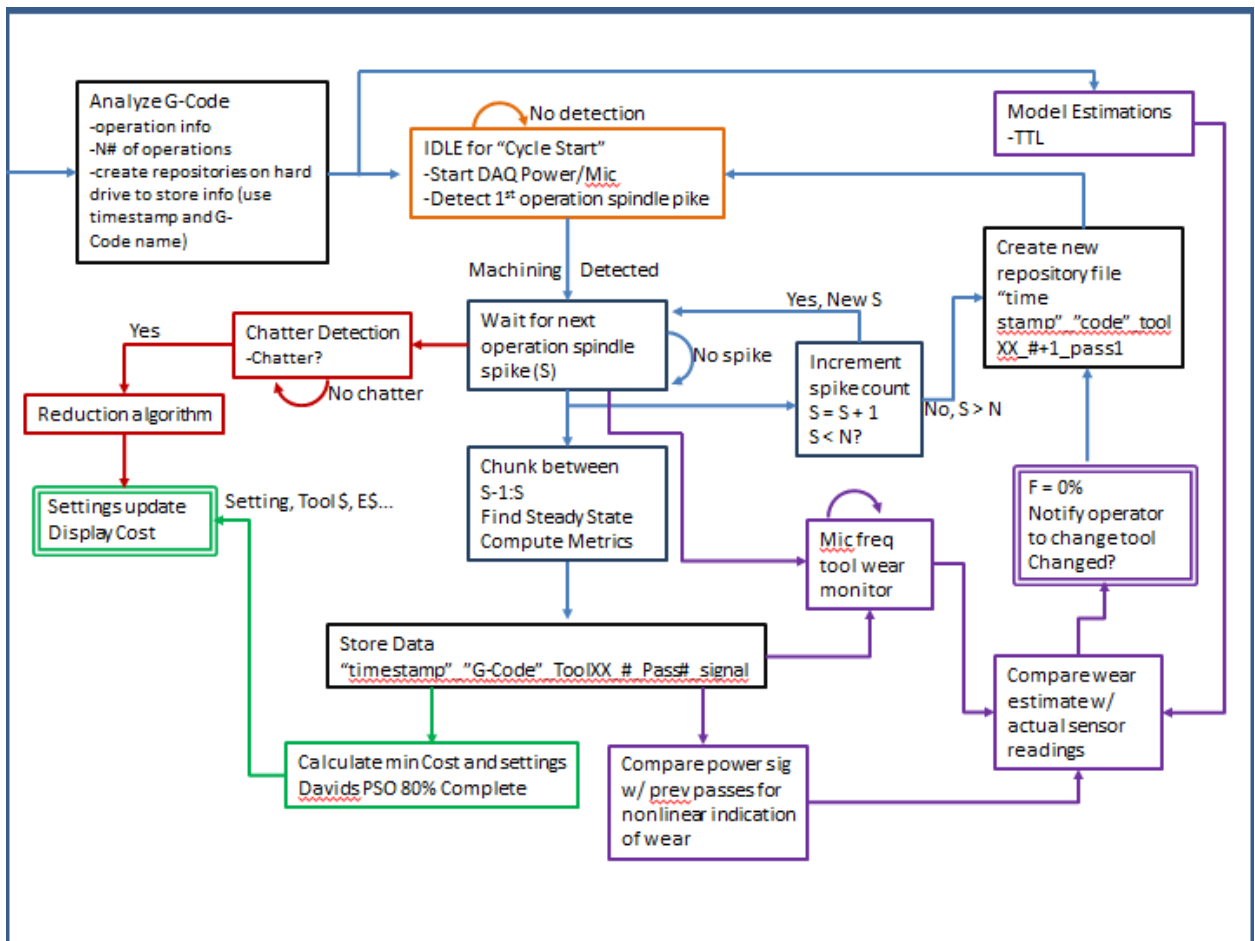


Figure 30: Functional Diagram of Monitoring System

CHAPTER SIX: CONCLUSION

The results bring up new questions such as how to decouple power in microphone responses between the turning and boring process. Another topic spurred by the research is the management of sensor data for an entire production floor with many machines. Is it more efficient for each machine to have its own independent monitoring system? The alternative is to have a central server that processes sensor data and sends commands back to the CNC. The arrival of cloud computing could be advantageous for a database management system.

The DoE method proved beneficial in understanding how the cost may be reduced by optimizing the process settings. The results presented in the paper suggest that the cost of machining may be reduced by changing the settings to 380 RPM and 0.022 IPR. A saving in energy consumption (kWh) by 11.8%, cutting time by 13.2% and a total cost reduction from \$1.15 per tool pass to \$1.075 per tool pass. The significant cost reduction is an effect of the offline optimization of multiple responses including the cutting time, energy consumption and tool life. This was done by successfully completing each step for a DoE study, from the beginning of applying sensor technology to the 1984 Okuma Turning Center to optimizing the settings and validating the results. The use of Labview to synchronize the acquisition of twenty one data signals from 10 Hz to 800 kHz is a major accomplishment of the project. The power meter and microphone analysis provide a foundation for retrofitting the 1984 Okuma Turning Center with a CNC monitoring system.

REFERENCES

- [1] I. A. Choudhury and M. A. El-Baradie, "Tool-life prediction model by design of experiments for turning high strength steel (290 BHN)," *Journal of Materials Processing Technology*, vol. 77, pp. 319-326, 1998.
- [2] Z. Yao, D. Mei, and Z. Chen, "On-line chatter detection and identification based on wavelet and support vector machine," *Journal of Materials Processing Technology*, vol. 210, pp. 713-719, 2010.
- [3] J. H. Lange and N. H. Abu-Zahra, "Tool Chatter Monitoring in Turning Operations Using Wavelet Analysis of Ultrasound Waves," *The International Journal of Advanced Manufacturing Technology*, vol. 20, pp. 248-254, 2002.
- [4] C. Scheffer, H. Kratz, P. S. Heyns, and F. Klocke, "Development of a tool wear-monitoring system for hard turning," *International Journal of Machine Tools and Manufacture*, vol. 43, pp. 973-985, 2003.
- [5] A. Ghasempour, J. Jeswiet, and T. N. Moore, "Real time implementation of on-line tool condition monitoring in turning," *International Journal of Machine Tools and Manufacture*, vol. 39, pp. 1883-1902, 1999.
- [6] S. Kurada and C. Bradley, "A review of machine vision sensors for tool condition monitoring," *Computers in Industry*, vol. 34, pp. 55-72, 1997.
- [7] D. S. Dimla E, "Sensor signals for tool-wear monitoring in metal cutting operations—a review of methods," *International Journal of Machine Tools and Manufacture*, vol. 40, pp. 1073-1098, 2000.
- [8] E. Kuljanic, M. Sortino, and G. Totis, "Multisensor approaches for chatter detection in milling," *Journal of Sound and Vibration*, vol. 312, pp. 672-693, 2008.
- [9] L. Xiaoli, "A brief review: acoustic emission method for tool wear monitoring during turning," *International Journal of Machine Tools and Manufacture*, vol. 42, pp. 157-165, 2002.
- [10] S. Dey and J. A. Stori, "A Bayesian network approach to root cause diagnosis of process variations," *International Journal of Machine Tools and Manufacture*, vol. 45, pp. 75-91, 2005.
- [11] J. Kopač and S. Šali, "Tool wear monitoring during the turning process," *Journal of Materials Processing Technology*, vol. 113, pp. 312-316, 2001.

- [12] D. Yan, T. I. El-Wardany, and M. A. Elbestawi, "A multi-sensor strategy for tool failure detection in milling," *International Journal of Machine Tools and Manufacture*, vol. 35, pp. 383-398, 1995.
- [13] S. Binsaeid, S. Asfour, S. Cho, and A. Onar, "Machine ensemble approach for simultaneous detection of transient and gradual abnormalities in end milling using multisensor fusion," *Journal of Materials Processing Technology*, vol. 209, pp. 4728-4738, 2009.
- [14] R. A. Fisher, *The design of experiments*: Hafner Pub. Co., 1966.
- [15] R. A. Fisher, *Statistical methods for research workers*: Oliver and Boyd, 1930.
- [16] K. Rekab and M. Shaikh, *Statistical design of experiments with engineering applications*: Taylor & Francis, 2005.
- [17] W. E. Deming, *Out of the crisis*: MIT Press, 2000.
- [18] L. W. Condra, *Reliability improvement with design of experiments*: Marcel Dekker, 2001.
- [19] T. L. Schmitz and K. S. Smith, *Machining Dynamics: Frequency Response to Improved Productivity*: Springer, 2008.
- [20] J. L. Myers, *Fundamentals of experimental design*: Allyn and Bacon, 1979.
- [21] S. Kalpakjian and S. R. Schmid, *Manufacturing engineering and technology*: Prentice Hall, 2006.
- [22] F. W. Taylor, *On the art of cutting metals*: The American society of mechanical engineers, 1907.
- [23] A. G. Atkins, *The science and engineering of cutting: the mechanics and processes of separating, scratching and puncturing biomaterials, metals and non-metals*: Butterworth-Heinemann, 2009.
- [24] (2010). *NIST/SEMATECH e-Handbook of Statistical Methods*. Available: <http://www.itl.nist.gov/div898/handbook/>
- [25] R. H. Myers, D. C. Montgomery, and C. M. Anderson-Cook, *Response surface methodology: process and product optimization using designed experiments*: Wiley, 2009.
- [26] J. W. Tukey, *Exploratory Data Analysis*: Addison-Wesley Pub. Co., 1977.

- [27] S. S. Rao, *Applied Numerical Methods for Engineers and Scientists*: Pearson Education, Limited, 2006.
- [28] M. J. Roberts and R. Russo, *A student's guide to analysis of variance*: Routledge, 1999.
- [29] G. Salvendy, *Handbook of industrial engineering: technology and operations management*: Wiley, 2001.
- [30] J. Tlusty, *Manufacturing processes and equipment*: Prentice Hall, 2000.
- [31] M. Y. Noordin, V. C. Venkatesh, S. Sharif, S. Elting, and A. Abdullah, "Application of response surface methodology in describing the performance of coated carbide tools when turning AISI 1045 steel," *Journal of Materials Processing Technology*, vol. 145, pp. 46-58, 2004.
- [32] T. Somkiat, "In-process monitoring and detection of chip formation and chatter for CNC turning," *Journal of Materials Processing Technology*, vol. 209, pp. 4682-4688, 2009.
- [33] H. Saglam, F. Unsacar, and S. Yaldiz, "Investigation of the effect of rake angle and approaching angle on main cutting force and tool tip temperature," *International Journal of Machine Tools and Manufacture*, vol. 46, pp. 132-141, 2006.
- [34] D. Shi and N. N. Gindy, "Development of an online machining process monitoring system: Application in hard turning," *Sensors and Actuators A: Physical*, vol. 135, pp. 405-414, 2007.